Fast and backward stable computation of roots of polynomials

Jared L. Aurentz *Thomas Mach* *Raf Vandebril*
David S. Watkins

Report TW 654, August 2014

KU Leuven
Department of Computer Science
Celestijnenlaan 200A – B-3001 Heverlee (Belgium)

Fast and backward stable computation of roots of polynomials

Jared L. Aurentz *Thomas Mach* *Raf Vandebril*
David S. Watkins

Report TW 654, August 2014

Department of Computer Science, KU Leuven

Abstract

A stable algorithm to compute the roots of polynomials is presented. The roots are found by computing the eigenvalues of the associated companion matrix by Francis's implicitly-shifted QR algorithm. A companion matrix is an upper Hessenberg matrix that is unitary-plus-rank-one, that is, it is the sum of a unitary matrix and a rank-one matrix. These properties are preserved by iterations of Francis's algorithm, and it is these properties that are exploited here. The matrix is represented as a product of $3n-1$ Givens rotators plus the rank-one part, so only $O(n)$ storage space is required. In fact, the information about the rank-one part is also encoded in the rotators, so it is not necessary to store the rank-one part explicitly. Francis's algorithm implemented on this representation requires only $O(n)$ flops per iteration and thus $O(n^2)$ flops overall. The algorithm is described, backward stability is proved under certain conditions on the polynomial coefficients, and an extensive set of numerical experiments is presented. The algorithm is shown to be about as accurate as the (slow) Francis QR algorithm applied to the companion matrix without exploiting the structure. It is faster than other fast methods that have been proposed, and its accuracy is comparable or better.

Keywords : polynomial, root, zero, companion matrix, eigenvalue, QR algorithm, rotators
MSC : Primary : 65F15 Secondary : 65H17, 15A18, 65H04.

FAST AND BACKWARD STABLE COMPUTATION OF ROOTS OF POLYNOMIALS *

JARED L. AURENTZ†, THOMAS MACH‡, RAF VANDEBRIL‡, AND DAVID S. WATKINS†

Abstract. A stable algorithm to compute the roots of polynomials is presented. The roots are found by computing the eigenvalues of the associated companion matrix by Francis's implicitly-shifted QR algorithm. A companion matrix is an upper Hessenberg matrix that is unitary-plus-rank-one, that is, it is the sum of a unitary matrix and a rank-one matrix. These properties are preserved by iterations of Francis's algorithm, and it is these properties that are exploited here. The matrix is represented as a product of $3n-1$ Givens rotators plus the rank-one part, so only $O(n)$ storage space is required. In fact, the information about the rank-one part is also encoded in the rotators, so it is not necessary to store the rank-one part explicitly. Francis's algorithm implemented on this representation requires only $O(n)$ flops per iteration and thus $O(n^2)$ flops overall. The algorithm is described, backward stability is proved under certain conditions on the polynomial coefficients, and an extensive set of numerical experiments is presented. The algorithm is shown to be about as accurate as the (slow) Francis QR algorithm applied to the companion matrix without exploiting the structure. It is faster than other fast methods that have been proposed, and its accuracy is comparable or better.

Key words. polynomial, root, companion matrix, eigenvalue, QR algorithm, rotators

AMS subject classifications. 65F15, 65H17, 15A18, 65H04

1. Introduction.

We describe a method for computing the *roots* of a monic polynomial $p(z)$ expressed in terms of the monomial basis, say

$$p(z) = z^n + a_{n-1}z^{n-1} + \cdots + a_1 z + a_0.$$

We will assume throughout this paper that $a_0 \neq 0$, since otherwise we can factor out z and reduce the degree of the polynomial. Like many others before us, we solve this problem by using Francis's implicitly-shifted QR algorithm[1] to compute the eigenvalues of the associated *companion* matrix

$$A = \begin{bmatrix} & & & -a_0 \\ 1 & & & -a_1 \\ & \ddots & & \vdots \\ & & 1 & -a_{n-1} \end{bmatrix}. \tag{1.1}$$

As the companion matrix is of Hessenberg form, one can directly apply Francis's algorithm [19, 20, 32] to retrieve the eigenvalues. This is what the `roots` command

*The research was partially supported by the Research Council KU Leuven, projects CREA-13-012 Can Unconventional Eigenvalue Algorithms Supersede the State of the Art, OT/11/055 Spectral Properties of Perturbed Normal Matrices and their Applications, CoE EF/05/006 Optimization in Engineering (OPTEC), and fellowship F+/13/020 Exploiting Unconventional QR Algorithms for Fast and Accurate Computations of Roots of Polynomials; by the DFG research stipend MA 5852/1-1; by the Fund for Scientific Research–Flanders (Belgium) project G034212N Reestablishing Smoothness for Matrix Manifold Optimization via Resolution of Singularities; and by the Interuniversity Attraction Poles Programme, initiated by the Belgian State, Science Policy Office, Belgian Network DYSCO (Dynamical Systems, Control, and Optimization).

†Department of Mathematics, Washington State University, Pullman, WA 99164-3113, USA; ({jaurentz,watkins}@math.wsu.edu).

‡Department of Computer Science, KU Leuven, Celestijnenlaan 200A, 3001 Leuven (Heverlee), Belgium; ({thomas.mach,raf.vandebril}@cs.kuleuven.be).

[1] In this paper the terms Francis's algorithm and QR algorithm will be used interchangeably.

in MATLAB® does. This method preserves the upper Hessenberg form but does not exploit other structures present in the companion matrix. Cleve Moler stated in 1991 [24], referring to this approach:

> This method might not be the best possible because it uses n^2 storage and n^3 time. An algorithm designed specifically for polynomial roots might use order n storage and n^2 time.

In recent years several methods that use $O(n)$ storage and $O(n^2)$ time have been devised (see § 2), all of which exploit the fact that a companion matrix can be decomposed into the sum of a unitary and a rank-one matrix. If one then applies a unitary similarity transformation on this sum, one ends up again with a unitary-plus-rank-one matrix. More precisely, taking the similarity determined by the implicit-shifted QR algorithm always leads to a Hessenberg matrix equal to the sum of a unitary and a rank-one matrix. This is the main theoretical idea behind all the fast QR algorithms for companion matrices, differing, however, significantly in the way the matrix is represented and how the algorithm is implemented.

Of the fast methods proposed up to this point, none have been proved to be backward stable. The method that we propose here is backward stable under suitable assumptions on the coefficients of the polynomial. Our method is faster than the other fast QR-based methods. Our Fortran codes can be downloaded from http://people.cs.kuleuven.be/raf.vandebril.

The article is organized as follows. Section 2 discusses earlier work in this area. Section 3 introduces some terminology and notational conventions that will aid in the presentation of the new method. Section 4 presents our new memory-efficient representation of unitary-plus-rank-one matrices, the QR algorithm itself is discussed in Section 5, and some implementation details are given in Section 6. Section 7 presents the stability analysis. We finish with our numerical experiments in Section 8.

2. Previous work. The research on fast companion algorithms was initiated by Bini, Daddi, and Gemignani [6] relying on the relation $A = A^{-H} + UV^*$, with A the iterates in the QR algorithm, and UV^* a rank two part. It is proved that the strictly upper triangular part of A stems from a rank three matrix. The authors rely solely on the low rank structure and present a memory efficient storage of Q and R needed to execute explicit QR steps, i.e., explicitly computing Q, R, and forming their product RQ. Unfortunately the representation is not robust. Large discrepancies between the sizes of the vectors generating the low rank parts are observed, a problem which one is unable to fully solve. Moreover, the explicit version of the QR algorithm can be considered as a drawback as typically additional memory and computational effort is required compared to an implicit approach.

In [7] Bini, Eidelman, Gemignani, and Gohberg develop an explicit QR algorithm operating directly on the Hessenberg matrix. They store the rank one part with two vectors and the unitary matrix via quasiseparable generators. The quasiseparable representation is, however, not able to retain the unitarity. To overcome this problem the authors enforce the unitarity by taking out the tiny error and using it to update the generators of the rank one part. This update is constructed in such a way that it does not destroy the Hessenberg structure.

Chandrasekaran, Gu, Xia, and Zhu [13] were the first to perform implicit QR steps directly on the QR factorization of the Hessenberg matrix, where the Q matrix is decomposed in rotators and the low rank structure of the upper triangular part of R is stored via the sequentially semiseparable representation which essentially equals the quasiseparable representation in this case. Even though the rank of R should

be bounded by 2, they admit 3 and require compression after each step to keep the rank numerically bounded by 3. Also in this paper focus lies on retaining the low rank structure imposed by the unitary and rank-one matrix, but no effort is put in retaining the unitarity itself.

In [15] Delvaux, Frederix, and Van Barel present an algorithm for block companion matrices. The approach resembles [13] as the QR factorization of the Hessenberg matrix is stored, but the R factor is now stored via a Givens-weight representation. Again the unitary-plus-low-rank structure deteriorates while running the QR algorithm. The authors propose a restoration technique based on a combination of the ones proposed in [13]: obtain the desired rank in R and [7]: restore the unitary structure. At the end both the unitary and low rank part are combined to compute the eigenvalues.

Van Barel, Vandebril, Van Dooren, and Frederix present in [27] a representation based on three sequences of rotators and a vector. Implicit QR steps are executed on the factorization directly and no compression steps are used to enforce any of the three structures. As a result one ends with a unitary-plus-rank-one matrix that approximates a Hessenberg matrix; numerical round off slightly perturbs the exact cancellation that should occur between the unitary and low rank part.

In [5] Bini, Boito, Eidelman, Gemignani, and Gohberg enhance their previous results from [7] and convert their explicit QR version to an implicit one. Two different representations are used in the implementation of the algorithm: in each iterate the unitary matrix is stored as a product of essentially 2×2 and 3×3 unitary matrices, to update this matrix under a QR step the quasiseparable representation of the unitary matrix is computed and utilized. In [11] Boito, Eidelman, Gemignani, and Gohberg enhance and simplify their implicit version by doing all computations directly on the quasiseparable representation of the unitary matrix, a compression technique is used to reduce the number of quasiseparable generators after a QR step to a minimum.

Recently, in [18] Eidelman, Gohberg, and Haimovici revisit the method from [13]. They also describe a factorization of the companion matrix using $3n-3$ rotations similar to what we propose in this paper. However, they keep the low-rank part explicitly and go back to a semiseparable representation of R for the description of the QR algorithm. They, further, do not provide numerical results.

For completeness we mention that besides the QR variants there is also an approach based on companion pencils [10] and there are fast non unitary GR algorithms [2, 3, 34], but they are potentially unstable. Other, QR related approaches tackle root finding problems of polynomials expressed in other bases, e.g., comrade or confederate matrices [17, 29].

3. Core transformations. Our method makes heavy use of rotators. In the interest of flexibility we will introduce a more general concept. A *core transformation* G_i is a nonsingular matrix that is identical to the identity matrix except in the 2×2 submatrix in the $(i:i+1, i:i+1)$ diagonal block, which is called the *active part* of the core transformation. We will consistently use the subscript i on a core transformation G_i to indicate the position of the active part. It follows that the core transformations G_i and G_j commute whenever $|i-j|>1$.

In some of our work [2, 3] we have made use of core transformations that are not unitary, but in this paper we will use only unitary ones. Thus, in this paper, the term *core transformation* will mean *unitary* core transformation. Givens rotators, with active parts of the form $\left[\begin{smallmatrix} c & -s \\ s & \bar{c}\end{smallmatrix}\right]$ with $|c|^2+s^2=1$ are core transformations, and so are Givens reflectors $\left[\begin{smallmatrix} c & s \\ s & -\bar{c}\end{smallmatrix}\right]$. We implemented our codes using rotators, but we could

equally well have used reflectors. In our initial description we will refer to generic core transformations, which could be rotators, reflectors, or any other kind of unitary core transformations.

It is well known (and easy to prove) that every $n \times n$ unitary upper Hessenberg matrix can be factored into a descending sequence of $n-1$ core transformations:

$$Q = Q_1 Q_2 \dots Q_{n-1}. \tag{3.1}$$

To simplify the notation, to clarify some equations, and to increase the readability of the algorithms we will frequently depict a core transformation as $\vec{\hookrightarrow}$, where the tiny arrows indicate the position of the active part. For example, for $n = 9$, the factorization (3.1) can be depicted as

$$Q = Q_1 Q_2 \cdots Q_{n-1} = \quad .$$

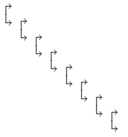

As another example, the equation

$$\vec{\hookrightarrow} \begin{bmatrix} x_1 \\ x_2 \\ x_3 \\ x_4 \end{bmatrix} = \begin{bmatrix} x_1 \\ x_2 \\ \tilde{x}_3 \\ 0 \end{bmatrix}$$

means that the vector x is multiplied by a core transformation G_3 on the left to produce a new vector that has a zero in the fourth position. With this notation established, we can now describe our new method.

4. Representation of the matrix. We will store each unitary-plus-rank-one upper Hessenberg matrix in QR decomposed form, as in [13]. Q is a unitary upper Hessenberg matrix, which can be stored compactly as a product of core transformations (3.1). R is an upper triangular unitary-plus-rank-one matrix. We decompose the latter into a unitary part and a rank-one part. All unitary matrices are stored as sequences of core transformations, as in [27]. We will prove that our representation of the unitary part also contains the information about the rank-one part encoded within the core transformations. Therefore there will be no need to keep track of or update the rank-one part in the course of the iterations. Everything will be updated automatically in the core transformations. Thus our algorithm will consist almost entirely of unitary similarity transformations on unitary matrices represented as products of core transformations.

Now we get more specific. Starting from a companion matrix, we begin by embedding it in a larger matrix

$$A = \left[\begin{array}{cccc|c} 0 & & & -a_0 & 1 \\ 1 & & & -a_1 & 0 \\ & 1 & & -a_2 & 0 \\ & & \ddots & & \vdots \\ & & 1 & -a_{n-1} & 0 \\ \hline & & 0 & 0 & 0 \end{array}\right], \tag{4.1}$$

with an extra row of zeros and column that is nearly zero. The one in the $(1, n+1)$ position ensures that the unitary-plus-rank-one structure is preserved. The enlarged

matrix clearly has one extra zero eigenvalue, which can be deflated out immediately. This curious beginning has at least three important consequences, as we shall see. It ensures that the information about the rank-one part is fully encoded in the core transformations. It results in a simpler, cleaner algorithm. Finally, it results in an algorithm that is backward stable.

If we take the QR factorization of the enlarged matrix, we obtain

$$Q = \left[\begin{array}{cccc|c} 0 & & & 1 & 0 \\ 1 & & & 0 & 0 \\ & 1 & & 0 & 0 \\ & & \ddots & \vdots & \vdots \\ & & 1 & 0 & 0 \\ \hline & & 0 & 0 & 1 \end{array}\right] \quad \text{and} \quad R = \left[\begin{array}{cccc|c} 1 & & & -a_1 & 0 \\ & 1 & & -a_2 & 0 \\ & & \ddots & \vdots & \vdots \\ & & 1 & -a_{n-1} & 0 \\ & & & -a_0 & 1 \\ \hline & & & 0 & 0 \end{array}\right].$$

We store Q as a product of core transformations as in (3.1). In this specific case we have $Q = Q_1 \cdots Q_{n-1}$ where each Q_i has active part $\left[\begin{smallmatrix} 0 & 1 \\ 1 & 0 \end{smallmatrix}\right]$. Here we are depicting the core transformations as reflectors for simplicity. In the actual code we used rotators $\left[\begin{smallmatrix} 0 & 1 \\ -1 & 0 \end{smallmatrix}\right]$, which can be done if we insert a factor $(-1)^{n-1}$ in appropriate entries in Q and R.

Since Q is of dimension $n+1$, the factorization into core transformations should have n factors, but in this case there are only $n-1$. The last transformation is trivial ($Q_n = I$) because the bottom row of A is trivial. This is important.

The upper triangular matrix has unitary-plus-rank-one form: $R = Z_n + xe_n^T$, where

$$Z_n = \left[\begin{array}{cccc|c} 1 & & & & \\ & 1 & & & \\ & & \ddots & & \vdots \\ & & & 1 & \\ \hline & & & 0 & 1 \\ & & & 1 & 0 \end{array}\right] \quad \text{and} \quad x = -\left[\begin{array}{c} a_1 \\ a_2 \\ \vdots \\ a_{n-1} \\ \hline a_0 \\ 1 \end{array}\right]. \tag{4.2}$$

Let $C_1, \ldots, C_n$ be core transformations such that $C_1 \cdots C_n x = \alpha e_1$, where $|\alpha| = \|x\|_2$. Pictorially, for $n = 8$, we have

$$\underbrace{\reflectbox{\rotatebox{90}{$\ddots$}}}_{C = C_1 \cdots C_n} \begin{bmatrix} x_1 \\ x_2 \\ x_3 \\ \vdots \\ x_{n+1} \end{bmatrix} = \begin{bmatrix} \alpha \\ 0 \\ 0 \\ \vdots \\ 0 \end{bmatrix}.$$

Let $C = C_1 C_2 \cdots C_n$. Since it is a product of a descending sequence of core transformations, C is a unitary upper Hessenberg matrix. Notice that since $|x_{n+1}| = 1 \neq 0$, the core transformation C_n is nontrivial (i.e. non diagonal). It follows easily that all of the C_i are nontrivial. Therefore C is a *proper* upper Hessenberg matrix, that is, its subdiagonal entries are all nonzero.

The information about the rank-one part is concentrated in the vector x. We form the C_i by *rolling up* x, transforming x to a multiple of e_1. In the process we are encoding the rank-one part in the core transformations C_i.

Letting $B = CZ_n$ and $y = \alpha e_n$, we have

$$R = C^*(B + e_1 y^T). \tag{4.3}$$

Notice that B is also a unitary upper Hessenberg matrix, so it can be factored into a product of a descending sequence of core transformations: $B = B_1 \cdots B_n$. In fact it is obvious that we can take $B_i = C_i$, for $i = 1, \ldots, n-1$, and $B_n = C_n Z_n$. Expanding (4.3) we have

$$R = C_n^* \cdots C_1^* (B_1 \cdots B_n + e_1 y^T).$$

Now combining Q and R, we have

$$A = QR = QC^*(B + e_1 y^T) = Q_1 \cdots Q_{n-1} C_n^* \cdots C_1^* (B_1 \cdots B_n + e_1 y^T). \tag{4.4}$$

Pictorially, for $n = 8$, we have

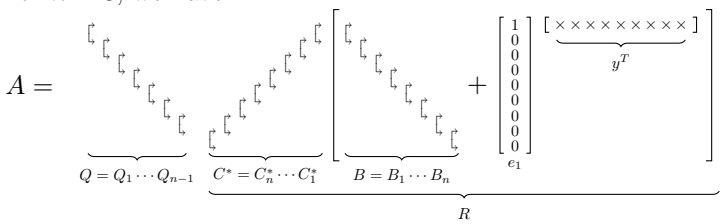

Notice that the Q sequence of core transformations is shorter than the other sequences due to the fact that the last row of A is trivial.

4.1. Properties of the factorization. The factorized form (4.4) is the form in which we will store our matrix. Over the course of the iterations of Francis's algorithm, the contents of the Q_i, C_i, B_i, and y will evolve, but the form (4.4) will be preserved. Certain specific properties of the form will be preserved as well, as we now show.

Although we are not yet ready to describe the algorithm, we can make some general statements about it. Because the last row of A represents a zero eigenvalue that has been deflated from the problem, the iterations of our algorithm will be similarity transformations by matrices of the form $U = \left[\begin{smallmatrix} \tilde{U} & 0 \\ 0 & 1 \end{smallmatrix}\right]$, where $\tilde{U}$ is $n \times n$. Initially we have $A = QR$, where $Q = \left[\begin{smallmatrix} \tilde{Q} & 0 \\ 0 & 1 \end{smallmatrix}\right]$ and $R = \left[\begin{smallmatrix} \tilde{R} & \times \\ 0 & 0 \end{smallmatrix}\right]$, and these general forms are preserved under such a similarity transformation, for (as we shall see) we have $\hat{A} = U^* A U = U^* Q R U = U^* Q V V^* R U = \hat{Q}\hat{R}$ for some unitary matrix V of the form $\left[\begin{smallmatrix} \tilde{V} & 0 \\ 0 & 1 \end{smallmatrix}\right]$. We have $R = Z + xz^T$, where x is initially given by (4.2). In particular $x_{n+1} = -1$. Under the transformation $R \to \hat{R} = V^* R U$, x is transformed to $\hat{x} = V^* x$. Because of the form of V, the transformed x still satisfies $x_{n+1} = -1$ and will continue to do so forever. Similarly the vector z is initially e_n, and in particular $z_{n+1} = 0$. This property will also persist. The vector y in (4.4) satisfies $y = \alpha z$, so we will have $y_{n+1} = 0$ forever.

Taking a closer look at the decomposition, we have $A = QC^*(B + e_1 y^T)$ and

$$\hat{A} = \hat{Q}\hat{C}^*(\hat{B} + e_1 \hat{y}^T) = (U^* Q V)(V^* C^* W)(W^* B U + e_1 y^T U), \tag{4.5}$$

where (as we shall see) the unitary W has a different form from the other transforming matrices: $W = \left[\begin{smallmatrix} 1 & 0 \\ 0 & \tilde{W} \end{smallmatrix}\right]$. This is the part of the algorithm in which row and column $n+1$ get used. Notice that $We_1 = e_1 = W^* e_1$, which justifies our leaving out the W^* that should have preceded the second e_1 in (4.5).

The equation $Cx = \alpha e_1$ holds initially, and we can now demonstrate that this relationship persists. We have $\hat{C}\hat{x} = (W^* C V)(V^* x) = W^* C x = \alpha W^* e_1 = \alpha e_1$.

Nontriviality of the core transformations C_i. We noted above that the core transformations $C_1, \ldots, C_n$ in (4.4) are all nontrivial initially. Now we can show that they remain nontrivial forever. This is a consequence of the following result, which we will also use in the stability analysis. Later on we will see that $B_1, \ldots, B_n$ are also nontrivial.

THEOREM 4.1. *For $i = 1, \ldots, n$, let $\left[\begin{smallmatrix} u_i & v_i \\ w_i & z_i \end{smallmatrix}\right]$ denote the active part of C_i in (4.4), and let $\gamma_i = |w_i| = |v_i|$. Then $\gamma_i > 0$, $i = 1, \ldots, n$. Moreover*

$$\gamma_1 \cdots \gamma_n = 1/\|x\|_2, \tag{4.6}$$

where x is given by (4.2).

Proof. The initial C_i satisfy $C_1 \cdots C_n x = \alpha e_1$, and we have noted just above that this relationship persists as the C_i and x evolve in the course of the iterations. The condition $x_{n+1} = -1$ also persists, and obviously $\|x\|_2$ remains invariant. Since $x = \alpha C_n^* \cdots C_1^* e_1$, we find by direct computation that $x_{n+1} = \alpha \overline{v}_n \cdots \overline{v}_1$. Taking absolute values we have $1 = |\alpha| \gamma_n \cdots \gamma_1$ or $\gamma_1 \cdots \gamma_n = 1/|\alpha| = 1/\|x\|_2$. ∎

Preservation of triangular and Hessenberg form. We want to know that the Hessenberg form is preserved by the iterations. To this end we must show that the triangular form of R is preserved.

THEOREM 4.2. *If the core transformations C_i in (4.4) are all nontrivial, then the matrix $R = C^*(B + e_1 y^T)$ is upper triangular.*

Proof. In the initial configuration we have $A = QR$, where

$$R = \begin{bmatrix} \tilde{R} & \times \\ 0 & 0 \end{bmatrix} \tag{4.7}$$

with $\tilde{R}$ of size $n \times n$, and $\times$ an insignificant vector. As we have noted above, this form of R persists during the iterations, so we just need to show that $\tilde{R}$ remains upper triangular. Since $R = C^*(B + e_1 y^T)$, we have $H = CR$, where $H = B + e_1 y^T$. We rewrite this equation in the partitioned form

$$\begin{bmatrix} \times & \times \\ \tilde{H} & \times \end{bmatrix} = \begin{bmatrix} \times & \times \\ \tilde{C} & \times \end{bmatrix} \begin{bmatrix} \tilde{R} & \times \\ 0 & 0 \end{bmatrix},$$

where $\tilde{H}$ and $\tilde{C}$ are both $n \times n$, and the $\times$ represent quantities that are not of immediate interest. The fact that the core transformations C_i are all nontrivial implies that C is a proper upper Hessenberg matrix ($c_{i+1,i} \neq 0$, $i = 1, \ldots, n$) which implies that $\tilde{C}$ is upper triangular and nonsingular. Similarly, $\tilde{H}$ is upper triangular. We note further that $\tilde{H} = \tilde{C}\tilde{R}$, which implies

$$\tilde{R} = \tilde{C}^{-1}\tilde{H}. \tag{4.8}$$

Since $\tilde{H}$ and $\tilde{C}^{-1}$ are upper triangular, $\tilde{R}$ must also be upper triangular. ∎

Remark 4.3. The matrices $\tilde{H}$ and $\tilde{C}$ are taken in part from row $n+1$ of H and C respectively. These matrices have a row $n+1$ because we added a row artificially. Had we not done so, we would not have been able to prove this theorem.

The equation $A = QR$ can also be written as

$$\begin{bmatrix} \tilde{A} & \times \\ 0 & 0 \end{bmatrix} = \begin{bmatrix} \tilde{Q} & 0 \\ 0 & 1 \end{bmatrix} \begin{bmatrix} \tilde{R} & \times \\ 0 & 0 \end{bmatrix}.$$

We have $\tilde{A} = \tilde{Q}\tilde{R}$, and it is on this submatrix that we principally operate. Because $a_0 \neq 0$, $\tilde{A}$ has no zero eigenvalues, so it is nonsingular.

THEOREM 4.4. *If the core transformations C_i in (4.4) are all nontrivial, then $\tilde{A}$ is upper Hessenberg. If $\tilde{A}$ is nonsingular, then $\tilde{A}$ is properly upper Hessenberg if and only if $\tilde{Q}$ is properly upper Hessenberg. Thus $\tilde{A}$ is properly upper Hessenberg if and only if $Q_1, \ldots, Q_{n-1}$ are all nontrivial.*

This tells us that a deflation will take place if and only if one of the Q_i becomes trivial.

Proof. Since $\tilde{R}$ is upper triangular and $\tilde{Q}$ is upper Hessenberg, $\tilde{A} = \tilde{Q}\tilde{R}$ must be upper Hessenberg. If $\tilde{A}$ is nonsingular, so is $\tilde{R}$. Thus $r_{ii} \neq 0$ for all i. Since $a_{i+1,i} = q_{i+1,i}r_{ii}$ for $i = 1, \ldots, n$, we see that $\tilde{A}$ is properly upper Hessenberg if and only if $\tilde{Q}$ is. ∎

Nontriviality of the core transformations B_i. Because of the assumption $a_0 \neq 0$ we can show that the core transformations B_i are also nontrivial.

THEOREM 4.5. *For $i = 1, \ldots, n$, let $\left[\begin{smallmatrix} u_i & v_i \\ w_i & z_i \end{smallmatrix}\right]$ denote the active part of B_i in (4.4), and let $\beta_i = |w_i| = |v_i|$. Then $\beta_i > 0$, $i = 1, \ldots, n$. Moreover*

$$\beta_1 \cdots \beta_n = |a_0|/\|x\|_2, \tag{4.9}$$

where x is given by (4.2).

Proof. The subdiagonal entries of the upper Hessenberg matrix $B = B_1 \cdots B_n$ are exactly the elements w_i, the subdiagonal entries of the active parts of the B_i. These are also the subdiagonal entries of $H = B + e_1 y^T$ and the main diagonal entries of the upper triangular submatrix $\tilde{H}$ defined in the proof of Theorem 4.2. By similar reasoning the main diagonal entries of $\tilde{C}$ are exactly the subdiagonal entries of the active parts of the C_i. Since $\tilde{H} = \tilde{C}\tilde{R}$ we have $h_{i+1,i} = c_{i+1,i}r_{ii}$ for $i = 1, \ldots, n$. Taking absolute values we have $\beta_i = \gamma_i |r_{ii}|$, where the γ_i are as defined in Theorem 4.1 . Now, taking a product, using Theorem 4.1, and noting that $|\det \tilde{R}| = |\det \tilde{A}| = |a_0|$, we have

$$\beta_1 \cdots \beta_n = \gamma_1 \cdots \gamma_n |\det \tilde{R}| = |a_0|/\|x\|_2.$$

∎

Extracting y from the core transformations. The representation of R in (4.4) has some redundancy. The information about the rank-one part is stored directly in y, but it is also encoded in the core transformations, as the following theorem shows. This justifies our claim that there is no need to keep track of the rank-one part.

THEOREM 4.6. *$y^T = -\rho^{-1} e_{n+1}^T C^* B$, where $\rho = e_{n+1}^T C^* e_1$. ρ is the product of the subdiagonal entries of $C_1^*, \ldots, C_n^*$, and therefore $|\rho| = 1/\|x\|_2$.*

Proof. The entire last row of R is zero. Therefore

$$0 = e_{n+1}^T R = e_{n+1}^T C^*(B + e_1 y^T) = e_{n+1}^T C^* B + e_{n+1}^T C^* e_1 y^T.$$

This can be solved for y^T to yield the desired result. The scalar $\rho = e_{n+1}^T C^* e_1$ is easily shown to be equal to the product of the subdiagonal entries of the rotators C_i^* by direct computation. Thus, by Theorem 4.1, $|\rho| = 1/\|x\|_2$. ∎

Computing entries of A. At certain points in the algorithm we need to compute elements of A explicitly. These are the shift computation, the computation of the transformation that starts each iteration, and the final eigenvalue computation. In the course of computing elements of A we must compute elements of R. For example,

for the transformation that starts an iteration in the double-shift case, we need the submatix

$$\begin{bmatrix} a_{11} & a_{12} \\ a_{21} & a_{22} \\ 0 & a_{32} \end{bmatrix},$$

and for this we need

$$\begin{bmatrix} r_{11} & r_{12} \\ 0 & r_{22} \end{bmatrix}.$$

We will use conventional shift strategies that require the submatrix

$$\begin{bmatrix} a_{n-1,n-1} & a_{n-1,n} \\ a_{n,n-1} & a_{n,n} \end{bmatrix}.$$

For this we need

$$\begin{bmatrix} r_{n-2,n-1} & r_{n-2,n} \\ r_{n-1,n-1} & r_{n-1,n} \\ 0 & r_{n,n} \end{bmatrix}.$$

In each case we need just a few entries of R on or near the main diagonal. The same is true in the final eigenvalue computation. For example, if we just need to compute a single eigenvalue located at a_{kk}, we need only r_{kk}. We will show that each of these computations can be done easily in $O(1)$ time. Interestingly, it turns out that we can perform the computations without explicitly computing any of the entries of y. The key is that the vector y is the unique choice for which $R = C^*(B + e_1 y^T)$ is upper triangular; in the following arguments we rely on the triangularity of R.

Suppose, for example, we want to compute r_{kk}. First consider the whole kth column.

$$Re_k = C^*(B + e_1 y^T)e_k = C^*(Be_k + e_1 y_k).$$

Note that $Be_k = B_1 \cdots B_k e_k$ because $B_{k+1} \cdots B_n$ leaves e_k fixed. Let

$$w = Be_k = B_1 \cdots B_k e_k = \begin{bmatrix} w_1 \\ \vdots \\ w_{k+1} \\ 0 \\ \vdots \end{bmatrix}.$$

We will see that we can avoid computing w, but suppose for the moment we do the computation. Let $v = w + e_1 y_k$, differing from w only in the first component. Then $Re_k = C^* v$. This vector has zeros from position $k + 1$ on down, and notice that the same must be true of $C_k^* \cdots C_1^* v$. This is so because $C_n^* \cdots C_{k+1}^*$ operates only on positions $k + 1$ through $n + 1$ and leaves the norm of this subvector fixed. Thus the subvector has to be zero to begin with. It follows that $Re_k = C_k^* \ldots C_1^* v$. Now

consider the situation just before we apply C_k^*:

$$t = C_{k-1}^* \cdots C_1^* v = \begin{bmatrix} r_{1k} \\ \vdots \\ \tilde{w}_k \\ w_{k+1} \\ 0 \\ \vdots \end{bmatrix}.$$

The entry in position $k+1$ is w_{k+1}. In fact w_{k+1} is determined by B_k (it is equal to the subdiagonal entry of B_k) and is left untouched by $B_{k-1}, \ldots, B_1, C_1^*, \ldots, C_{k-1}^*$. Now consider the application of the final core transformation: $C_k^* t = Re_k$. Focusing on the interesting part, and abusing notation slightly, we have

$$C_k^* \begin{bmatrix} \tilde{w}_k \\ w_{k+1} \end{bmatrix} = \begin{bmatrix} r_{kk} \\ 0 \end{bmatrix}.$$

If we temporarily write $\left[\begin{smallmatrix} a & b \\ c & d \end{smallmatrix}\right]$ for the active part of C_k^*, we have

$$\begin{array}{rcl} a\tilde{w}_k + bw_{k+1} & = & r_{kk} \\ c\tilde{w}_k + dw_{k+1} & = & 0. \end{array}$$

Solving the second equation for the unknown $\tilde{w}_k$, we have $\tilde{w}_k = -dw_{k+1}/c$. Substituting this value back into the first equation, we get

$$r_{kk} = \frac{-ad+bc}{c} w_{k+1} = \frac{-\det(C_k)}{c} w_{k+1}.$$

The determinant of C_k is a number of unit modulus. In our implementation we will always use rotators as our core transformations. Since these have determinant 1, we get in this case the very satisfying formula

$$r_{kk} = -w_{k+1}/c. \tag{4.10}$$

The numbers w_{k+1} and c are the subdiagonal entries of rotators B_k and C_k^*, respectively. We conclude that the computation of r_{kk} costs exactly one division. The number y_k, which appeared briefly in the discussion, is not needed.

Now suppose we also need $r_{k-1,k}$. We can use the same technique as above, but we need to generate a bit more of the vector w. The entries w_k and w_{k+1} are determined entirely by B_k and B_{k-1}. Looking at the interesting part of the computation, and abusing notation slightly, we have

$$B_{k-1}B_k \begin{bmatrix} 0 \\ 1 \\ 0 \end{bmatrix} = \begin{bmatrix} \hat{w}_{k-1} \\ w_k \\ w_{k+1} \end{bmatrix}.$$

Letting $v = w + e_1 y_k$ as before, consider again the computation $C^* v = C_k^* \cdots C_1^* v = Re_k$. Before the final application of $C_k^* C_{k-1}^*$ we have

$$t = C_{k-2}^* \cdots C_1^* v,$$

where the interesting part of t has the form $[\tilde{w}_{k-1}\ w_k\ w_{k+1}]^T$. The entries w_k and w_{k+1} were created by B_k and B_{k-1} and left untouched by $B_{k-2}\ \ldots,\ B_1,\ C_1^*,\ \ldots,\ C_{k-2}^*$. Now, completing the computation, focusing on the interesting part, we have

$$C_k^* C_{k-1}^* \begin{bmatrix} \tilde{w}_{k-1} \\ w_k \\ w_{k+1} \end{bmatrix} = \begin{bmatrix} r_{k-1,k} \\ r_{k,k} \\ 0 \end{bmatrix}.$$

This is a system of three equations, the last of which can be solved for the unknown $\tilde{w}_{k-1}$. This value can then be substituted back into the first equation to yield a formula for $r_{k-1,k}$. We leave it to the reader to develop the explicit formula. The cost of the computation is $O(1)$. It uses only B_k, B_{k-1}, C_{k-1}^*, and C_k^*, and does not need y_k.

If we also need $r_{k-2,k}$, we do just a bit more work. We have

$$B_{k-2}B_{k-1}B_k \begin{bmatrix} 0 \\ 0 \\ 1 \\ 0 \end{bmatrix} = \begin{bmatrix} \hat{w}_{k-2} \\ w_{k-1} \\ w_k \\ w_{k+1} \end{bmatrix}$$

and

$$C_k^* C_{k-1}^* C_{k-2}^* \begin{bmatrix} \tilde{w}_{k-2} \\ w_{k-1} \\ w_k \\ w_{k+1} \end{bmatrix} = \begin{bmatrix} r_{k-2,k} \\ r_{k-1,k} \\ r_{k,k} \\ 0 \end{bmatrix}.$$

We solve the last equation for $\tilde{w}_{k-2}$, then substitute back into the first equation to get a formula for $r_{k-2,k}$. Again we leave the details to the reader.

It follows from these considerations that, once we have the matrix written in the factored from (4.4), we never have to refer back explicitly to the rank-one part of the matrix.

5. The algorithm. We now consider how to execute single and double steps of Francis's implicitly shifted QR algorithm [30] by directly operating on the factored form (4.4). In a standard QR step we disturb the Hessenberg structure by introducing a bulge at the top of the matrix, which is then chased by unitary similarity transformations to the bottom of the Hessenberg matrix until it slides off the matrix. For a detailed description see [31].

In our setting the bulge is represented by extra core transformations that are introduced and then chased through the factored form. First, we disturb the factorization by introducing the bulge (Sections 5.2 and 5.5, for the single and double shift respectively), then we restore the factorization by chasing the bulge via unitary similarity transformations (Sections 5.2 and 5.5) until it disappears (Sections 5.4 and 5.7).

The algorithm utilizes two simple operations on core transformations called *fusion* and *turnover*. Two core transformations acting on the same rows can be *fused* into a single one,

One can also change a factorization of core transformations between the following two forms

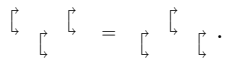

This is the *turnover* operation, and it can be done in either direction. This is proved easily by thinking of computing the QR factorization of a 3×3 unitary matrix using, say, Givens rotations. (The R matrix is trivial.) It is also convenient to look at the turnover differently. Consider a core transformation on the right of an ascending sequence. One can pass it through the sequence by a single turnover, and a new core transformation pops up on the left, positioned on row above its original position (the vertical lines have no meaning except to pinpoint the interesting spots in the figure):

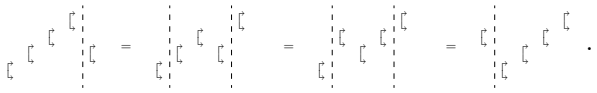

Similarly one can pass a core transformation from right to left through a descending sequence, thereby moving it down a single row.

5.1. Deflations and properness. The QR algorithm operates on proper Hessenberg matrices, i.e., all subdiagonal elements are nonzero. Obviously, when zeros do appear on the subdiagonal, one can decouple the original problem into Hessenberg matrices of lesser size and compute their eigenvalues. This process is called deflation. Common criteria to check whether a subdiagonal element numerically equals zero check whether the subdiagonal entries of the upper Hessenberg matrix are sufficiently small. When considering, however, the matrix in the factored form (4.4), we see that a deflation is signaled by an almost diagonal core transformation Q_i (Theorem 4.4). Rather than explicitly computing all subdiagonal elements of the Hessenberg matrix, we will check for deflations by examining the Q_i. If a subdiagonal entry is below the unit roundoff, we deflate. It is proved in [23] that a deflation via core transformations of a single eigenvalue provides good relative backward error.

Once a deflation has occurred, we must operate on submatrices of the original matrix. This presents no difficulties, and we omit the details.

5.2. Single shift: introducing the bulge. We begin by computing a shift μ by a standard shifting strategy (Section 6). For this we need to construct the 2×2 submatrix in the lower-right-hand corner of A. We can do this in $O(1)$ flops as we have seen in Section 4.1.

Then we must compute a vector $v = (A - \mu I)e_1$, for which we need a_{11} and a_{21}. We can compute these once we have r_{11}, which we obtain in one division as shown in Section 4.1. Only the first two entries of v are nonzero. Let U_1 be a core transformation with first column proportional to v, i.e. $U_1 e_1 = \gamma(A - \mu I)e_1$, and perform a similarity transform with U_1. The resulting matrix $U_1^* A U_1$ can be pictured as

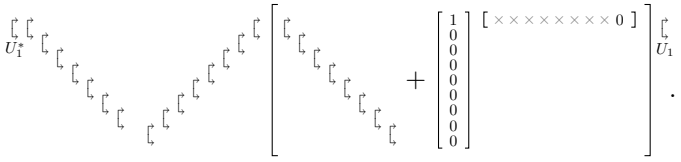

Clearly we can get rid of U_1^* by fusing it with Q_1. Then the representation is in the desired form, except for the core transformation U_1 on the right. This is the

bulge. We must chase it through the matrix from right to left, from top to bottom, until it gets absorbed by fusion.

5.3. Single shift: chasing the bulge. We chase U_1 from right to left. First U_1 is applied on both terms in the factor $B+e_1y^T$; we get $(B+e_1y^T)U_1 = BU_1+e_1y^TU_1 = BU_1 + e_1\tilde{y}^T$. As B is a descending sequence of core transformations, we can pass U_1 through it by a single turnover, moving it down one position. We get $BU_1 = \hat{U}_2\tilde{B}$. Pictorially we get (5.1), where each individual arrow corresponds to a specific action to bring the core transformation U_1 more and more to the left. More precisely, we start with the two arrows leaving U_1 on the right. The top arrow expresses that U_1 is applied to y^T thereby transforming y into $\tilde{y}$. The bottom arrow moves U_1 inside the brackets, to the right of B. The arrow starting from U_1 next to B indicates that the next step is to move U_1 to the left through the descending sequence by a turnover. As a result we get $\hat{U}_2$, and B becomes $\tilde{B}$.

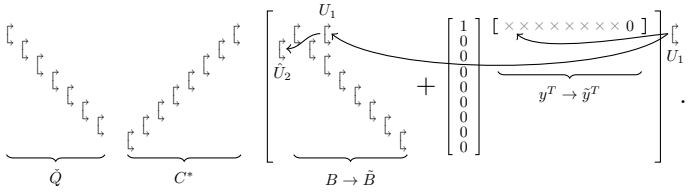

(5.1)

In our illustrations we are displaying the rank-one part for completeness, but it is important to remember that in our code we do not store or update y explicitly. The information about y is encoded in the B and C core transformations, as explained in Theorem 4.6. Whenever we need information about the rank-one part, we extract it from the core transformations as shown in Theorem 4.6.

The core transformation $\hat{U}_2$ can be moved outside the brackets without affecting the rank one part as it does not touch the first row:

$$C^*(\hat{U}_2\tilde{B} + e_1\tilde{y}^T) = C^*\hat{U}_2(\tilde{B} + e_1\tilde{y}^T).$$

($\hat{U}_2$ will become part of the matrix W mentioned in (4.5).)

To bring the bulge $\hat{U}_2$ completely to the left we pass it through the ascending sequence C^* by an upward turnover, moving it up a row and giving $\check{U}_1$. ($\check{U}_1$ becomes part of the matrix V in (4.5).) Then we pass it through the descending sequence Q, moving it back down a row, resulting in U_2.

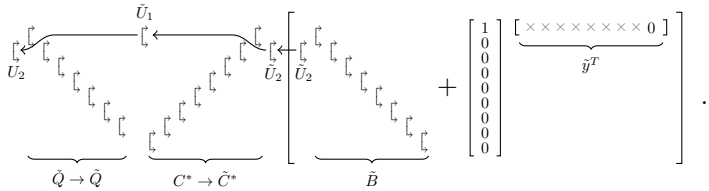

Now perform a similarity transformation by U_2. In the resulting matrix

$$U_2^*U_1^*AU_1U_2,$$

the bulge U_2 has disappeared from the left and shown up on the right. We then pass U_2 through the matrix in exactly the same way as we did with U_1, resulting in a new, lower positioned, core transformation U_3 on the left. We then do a similarity transformation by U_3, moving it from the left to the right, pass it through the matrix again to obtain U_4, and so on. After $n-2$ steps we arrive at the bottom.

5.4. Single shift: absorbing the bulge, end of the chase. The next figure illustrates the final pass through the matrix.

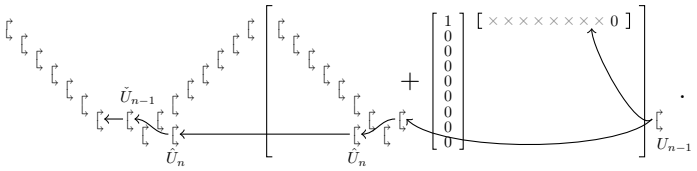

We pass U_{n-1} through the descending B sequence to produce $\hat{U}_n$, which is then passed through the ascending C^* sequence to produce $\check{U}_{n-1}$. Because the descending Q sequence is shorter than the others, it is now possible to fuse $\check{U}_{n-1}$ with Q_{n-1}. Once we do this, we have eliminated the bulge. We have returned the matrix to the form (4.4) so, by Theorem 4.4, Hessenberg form has been restored.

The entire similarity transformation is $\hat{A} = U^*AU$, where $U = U_1U_2\cdots U_{n-1}$. The core transformations $U_2, \ldots, U_{n-1}$ all satisfy $U_ie_1 = e_1$, so $Ue_1 = U_1e_1 = \gamma(A - \mu I)e_1$. We have effected a unitary similarity transformation from proper Hessenberg form to Hessenberg form with the "right" first column. Therefore we have executed an iteration of Francis's algorithm [30, Theorem 4.5.5], [31, Theorems 5.6.14, 6.3.12].

Notice that in the final step we created briefly a core transformation $\hat{U}_n$ that occupies rows/columns n and $n+1$. Row and column $n+1$ would not exist if we had not artificially adjoined them at the beginning. Because of the immediate deflation of the added zero eigenvalue, the Q sequence of core transformations is shorter than the others, allowing us to terminate the bulge chase with a fusion in Q_{n-1}.

Remark 5.1. Early versions of our algorithm did not include the added row and column. As a consequence the bulge chase terminated prematurely with a fusion in the B sequence instead of the Q sequence. This meant that Hessenberg form had not been reached. To finish the operation we had to look into the R matrix and force one last entry to zero. For this purpose we needed to make use of the y vector, which we had to keep track of explicitly. This situation persisted until the first deflation was achieved, after which it became possible to complete the iteration without taking special action. (We also noticed that from that point on we had no further need to keep track of the y vector.) By adding an extra row and column with an artificial deflation, we were able to eliminate these complications.

5.5. Double shift: introducing the bulge. In the single shift algorithm the bulge is represented by a single core transformation. In the double shift code three core transformations are needed to represent the bulge, but it turns out that we only need to pass two at a time through the matrix.

We begin by obtaining two shifts μ_1 and μ_2 by a standard shifting strategy. Then we compute the vector $v = (A-\mu_1 I)(A-\mu_2 I)e_1$, which has only the first three entries nonzero. Let V_2 and U_1 be two core transformations such that $U_1^*V_2^*v = \gamma^{-1}e_1$ for some γ, so that $V_2U_1e_1 = \gamma v$. Then carry out a similarity transformation to produce $U_1^*V_2^*AV_2U_1$. Pictorially we have

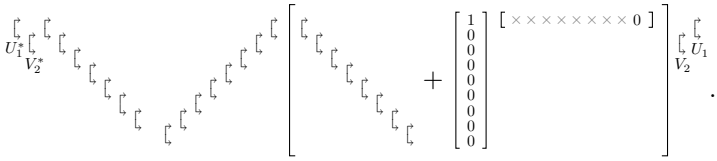

On the left side of the picture perform a turnover of $U_1^*V_2^*Q_1$ to produce $W_2\hat{Q}_1\check{Q}_2$. Then fuse $\check{Q}_2$ with Q_2 to form $\hat{Q}_2 = \check{Q}_2Q_2$. We now have

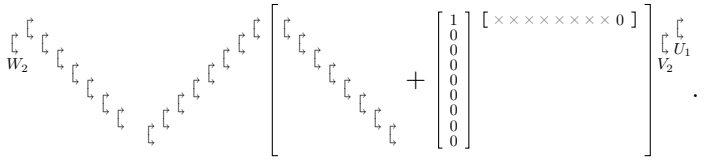

5.6. Double shift: chasing the bulge. In each chasing step we will bring both core transformations on the outer right to the outer left and execute a similarity to swap them back to the right. After the similarity we end up again with two core transformations on the right and a single one on the left, all positioned one row lower than before.

Let us illustrate the flow graphically. Moving the two right core transformations to the left proceeds identically to the single shift case: apply them to the two terms, pass them through the B sequence, bring them outside the brackets, pass them through the C^* sequence, and finally go through the Q sequence to arrive on the left side. Because V_2 is positioned to the left of U_1, V_2 should go first. We get

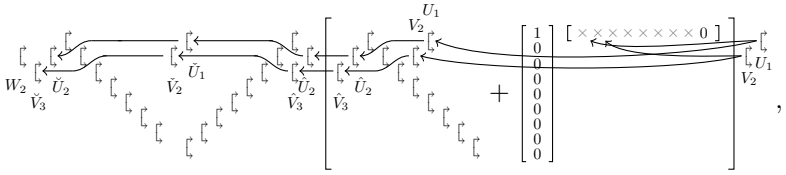

Now do a turnover of $W_2\check{V}_3\check{U}_2$ to produce $V_3U_2W_3$. Then do a similarity transformation with V_3U_2 to move those two core transformations from the left side to the right. This concludes the first chasing step. The next step is identical to the first, except that everything has been moved down by one.

We remind the reader that, although we are showing the rank-one part in the pictures for completeness, we do not actually store or update y explicitly.

5.7. Double shift: absorbing the bulge, end of the chase. After $n-3$ chasing steps the core transformations reach the bottom of the matrix, where they will be absorbed. We will graphically depict what happens to core transformations V_{n-1} and U_{n-2} individually. First V_{n-1} goes through the B and C^* sequences and fuses with the bottom core transformation in the Q sequence:

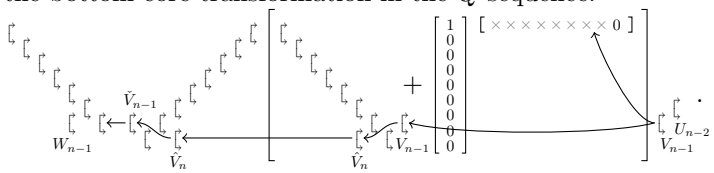

Then bring core transformation U_{n-2} through the B, C^*, and Q sequences, where it can be fused with W_{n-1} leaving a single core transformation U_{n-1} on the left.

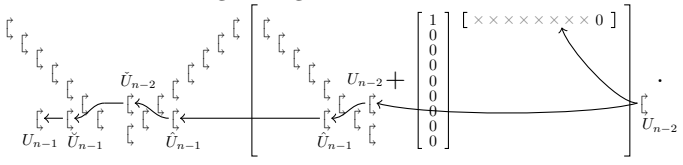

Perform a similarity transformation with U_{n-1} to move it from the left side to the right. Then pass it through the matrix one more to time and fuse it with the bottom core transformation in the Q sequence, exactly as in the single shift case. The bulge has been absorbed. We have returned the matrix to the form (4.4), and the iteration is complete.

The entire similarity transformation is $\hat{A} = U^* A U$, where

$$U = V_2 U_1 V_3 U_2 \cdots V_{n-1} U_{n-2} U_{n-1}.$$

Since $U_i e_1 = e_1$ and $V_i e_1 = e_1$ for $i > 1$, we have

$$U e_1 = V_2 U_1 e_1 = \gamma (A - \mu_1)(A - \mu_2) e_1.$$

We have effected a unitary similarity transform with the "right" first column, transforming a properly upper Hessenberg matrix to an upper Hessenberg matrix. Therefore we have executed a Francis iteration of degree two [30, Theorem 4.5.5], [31, Theorems 5.6.14, 6.3.12].

6. Implementation. Two versions of the algorithm are implemented in Fortran 90. There is the *complex single shift* (CSS) code to retrieve the roots of complex polynomials, and the *real double shift* (RDS) code to stick to real arithmetic when dealing with real polynomials. In the next sections we briefly discuss the storage scheme, the basic operations, and the heuristics used.

6.1. Data storage. As core transformations we took rotators with real s,

$$\begin{bmatrix} c & -s \\ s & \overline{c} \end{bmatrix}, \tag{6.1}$$

where $|c|^2 + s^2 = 1$. Three sequences of these rotators, of which only c and s are required, need to be stored.

In the RDS code all core transformations are real and remain so during the iterations. Both c and s are reals, leading to a storage cost of roughly $6n$ reals.

In the CSS setting, if one wishes to keep the s entries real, more effort is required. This restriction demands that we start with an upper Hessenberg matrix whose subdiagonal entries are all real. This can always be arranged and is already fulfilled for companion matrices. In Section 6.2 we will see that the turnover will not cause problems, only the fusion does. Fusing core transformations with real s results in a single core transformation for which the s value is typically not real. This problem can be remedied by including an extra unitary diagonal matrix D in the Q factor: $Q = Q_1 \cdots Q_{n-1} D$, where D contains some phase factors. Details are given below. The actual factored form utilized in the CSS code is therefore

$$A = QR = (Q_1 \cdots Q_{n-1}) D (C_n^* \cdots C_1^*)(B_1 \cdots B_n + \alpha e_1 y^T).$$

As a result we need to store a complex c, stored as two reals, and a real s for each core transformation. The diagonal D is complex, each element takes up two reals. In total we get a storage cost of approximately $11n$ reals.

6.2. Operations. The next paragraphs describe how to execute a fusion, a turnover, and pass a core transformation through a diagonal for both the CSS and RDS codes.

Turnover. Executing a turnover is equivalent to computing a QR factorization of

$$\begin{bmatrix} c_1 & -s_1 & \\ s_1 & \overline{c}_1 & \\ & & 1 \end{bmatrix} \begin{bmatrix} 1 & & \\ & c_2 & -s_2 \\ & s_2 & \overline{c}_2 \end{bmatrix} \begin{bmatrix} c_3 & -s_3 & \\ s_3 & \overline{c}_3 & \\ & & 1 \end{bmatrix}$$

$$= \begin{bmatrix} c_1 c_3 - s_1 c_2 s_3 & -c_1 s_3 - s_1 c_2 \overline{c}_3 & s_1 s_2 \\ s_1 c_3 + \overline{c}_1 c_2 s_3 & -s_1 s_3 + \overline{c}_1 c_2 c_3 & -\overline{c}_1 s_2 \\ s_2 s_3 & s_2 c_3 & \overline{c}_2 \end{bmatrix} = \quad .$$

The first two rotators are computed from the first column. After updating the last column we can compute the final rotator. As a result we can simply ignore the second column. Rotators creating zeros in entries can always be chosen such to have real s, as a consequence the turnover keeps the real s's intact.

Passing a rotator through a diagonal. In the CSS code we also need to accomplish

$$\begin{bmatrix} d & 0 \\ 0 & e \end{bmatrix} \begin{bmatrix} c_1 & -s_1 \\ s_1 & \overline{c}_1 \end{bmatrix} = \begin{bmatrix} c_2 & -s_2 \\ s_2 & \overline{c}_2 \end{bmatrix} \begin{bmatrix} f & 0 \\ 0 & g \end{bmatrix}.$$

To this end take $f = e$, $g = d$, $s_2 = s_1$, and $c_2 = c_1 d\,\overline{e}$.

Fusion. We have

$$\begin{bmatrix} c_1 & -s_1 \\ s_1 & \overline{c}_1 \end{bmatrix} \begin{bmatrix} c_2 & -s_2 \\ s_2 & \overline{c}_2 \end{bmatrix} = \begin{bmatrix} c_1c_2 - s_1s_2 & -s_1c_2 - \overline{c}_1s_2 \\ s_1\overline{c}_2 + c_1s_2 & \overline{c}_1\overline{c}_2 - s_1s_2 \end{bmatrix} = \begin{bmatrix} c'_3 & -\overline{s'}_3 \\ s'_3 & \overline{c'}_3 \end{bmatrix},$$

where $s'_3 = s_1\overline{c}_2 + c_1s_2$ is not necessarily real when dealing with complex numbers (in the RDS case there are no issues). As a consequence the diagonal D is involved in a fusion in the CSS code, We compute

$$\begin{bmatrix} c'_3 & -\overline{s'}_3 \\ s'_3 & \overline{c'}_3 \end{bmatrix} = \begin{bmatrix} c_3 & -s_3 \\ s_3 & \overline{c}_3 \end{bmatrix} \begin{bmatrix} f & 0 \\ 0 & g \end{bmatrix},$$

which is realized by setting $s_3 = |s'_3|$, $\phi = s'_3/s_3$, $c_3 = c'_3\phi$, $f = \phi$, and $g = \overline{\phi}$. The values f and g are then incorporated into the diagonal D.

6.3. Heuristics and tunings.

Shift strategy. The *Wilkinson shift* [33] and the *Rayleigh quotient shift* are the most popular shift strategies for single and double shift QR algorithms. For the RDS code the eigenvalues of the trailing 2×2 submatrix under consideration are used as shifts, which are Rayleigh quotient shifts. This ensures that we can stick to real arithmetic during the entire QR algorithm. In the CSS case the Wilkinson shift, i.e. the eigenvalue of the trailing 2×2 block closest to the last diagonal element of the matrix under consideration, is used.

Deflation. A rotator is assumed to signal a deflation if $|s| < \epsilon_m \approx 2.22 \cdot 10^{-16}$, where ϵ_m stands for the machine precision. In the CSS code the rotator is set explicitly to the identity and the unimodular factors are put in the diagonal matrix D. In the RDS the rotator is explicitly set to a diagonal matrix with ± 1 on its diagonal.

We search for deflations starting at the bottom of the matrix. After a deflation the iterations are executed on the above positioned proper Hessenberg matrix larger than 2×2. The eigenvalues of 2×2 blocks are explicitly computed via the modified quadratic formula.

Square roots. During the turnover, the fusion, and the passing through a diagonal we have to ensure that the computed rotations fulfill $|c|^2 + s^2 = 1$. Thus the triplet (c_{real}, c_{imag}, s) or the pair (c, s) need to be renormalized. A square root is computationally very expensive and therefore the square root of η, with $\eta = c_{real}^2 + c_{imag}^2 + s^2$ or $\eta = c^2 + s^2$, is only computed if If $|\eta - 1| < \epsilon$, otherwise $\sqrt{\eta} = 1$. The value of ϵ is set to ϵ_m, but reducing it to, e.g., $\epsilon = 3 \cdot 10^{-14}$ saves a third of the computing time at the price of 2 significant digits. This trick, using $\epsilon = \epsilon_m$, saves about 30% of the computing time.

Exploiting $C_i = B_i$ in early stages. In the first iteration $B_i = C_i$ for $i = 1, \ldots, n-1$. After each iteration the number of coinciding rotators decreases by one. Exploiting this by saving the number of turnovers explicitly executed saves approximately 10% of the computing time.

7. Backward stability. Our analysis will push the error back onto the companion matrix, not onto the coefficients of the polynomial. For the latter we refer the reader to [14, 16, 28].

We begin by noting that our initial factorization $A = QR = QC^*(B + e_1y^T)$ is backward stable. That is, the exact matrix $QC^*(B + e_1y^T)$ differs from A by an amount that is on the order of the unit roundoff multiplied by $\|A\|_2$. This follows from elementary considerations. In particular, operations by Givens rotators are backward stable [21].

Now it suffices to show that a single step of the algorithm is backward stable. In exact arithmetic we have $\hat{A} = U^*AU$, and we want to show that in floating point the computed $\hat{A}$ satisfies $\hat{A} = U^*(A + E)U$, where $\|E\|$ is tiny relative to $\|A\|$. We consider the unitary and rank-one parts separately. $A = A_u + A_r$, where $A_u = QC^*B$ and $A_r = QC^*e_1y^T$. We easily deal with the unitary part. We should get $\hat{Q}\hat{C}^*\hat{B} = U^*QC^*BU$, but in practice we get $\hat{Q}\hat{C}^*\hat{B} = U^*(QC^*B + E_1)U$, where $\|E_1\|_2$ is a modest multiple of the unit roundoff. This is so because the entire transformation consists of a sequence of turnovers, fusions, and renormalizations. The fusion operation is a matrix-matrix multiply, which is backward stable [21]. The turnover can be viewed as two matrix-matrix multiplies followed by a QR factorization by rotators. Since the QR factorization is also backward stable [21], we deduce that the turnover is backward stable. Each renormalization operation introduces tiny errors on the order of the unit roundoff. These translate into tiny backward errors. Thus we have $\hat{A}_u = U^*(A_u + E_1)U$, where $\|E_1\|_2$ is a modest multiple of the unit roundoff. There is no complicating factor like $\|A\|_2$ because all of the matrices involved are unitary and therefore have norm 1.

The analysis of the rank-one part is more challenging. In exact arithmetic we have $\hat{Q}\hat{C}^*e_1\hat{y}^T = U^*QC^*e_1y^TU$ or $\hat{A}_r = U^*A_rU$, and we want to show that the computed quantities satisfy $\hat{A}_r = U^*(A_r + E_2)U$, where $\|E_2\|_2$ is small.

The vector y is not stored explicitly. Instead it is encoded implicitly in the core transformations that comprise B and C. The value of y is deduced Theorem 4.6. Referring to that theorem, we see that $y^T = \mp\|x\|_2e_{n+1}^TC^*B$, so

$$A_r = \mp\|x\|_2QC^*e_1e_{n+1}^TC^*B = \mp\|x\|_2A_u(B^*e_1)(e_{n+1}^TQ^*)A_u.$$

We have grouped the terms this way because we already know we have a good backward error result for the product $QC^*B = A_u$. From this factorization we see that we also need backward error results for Q and B separately. These are more difficult.

Recall that in exact arithmetic we have

$$\hat{A} = \hat{Q}\hat{C}^*(\hat{B} + e_1\hat{y}^T) = (U^*QV)(V^*C^*W)(W^*BU + e_1y^TU),$$

and in particular (in exact arithmetic)

$$\hat{Q} = U^*QV, \qquad \hat{B} = W^*BU, \qquad \text{and} \qquad \hat{C} = W^*CV.$$

Suppose we are able to obtain, for the computed quantities, results like

$$\hat{Q} = U^*(Q + E_3)V \qquad \text{and} \qquad \hat{B} = W^*(B + E_4)U$$

where $\| E_3 \|_2$ and $\| E_4 \|_2$ are small. Then we would have, for the computed quantities,

$$\begin{aligned}
\hat{A}_r &= \mp \| x \|_2 \hat{A}_u (\hat{B}^* e_1)(e_{n+1}^T \hat{Q}^*) \hat{A}_u \\
&= \mp \| x \|_2 U^* (A_u + E_1) U (U^* (B^* + E_4^*) W e_1)(e_{n+1}^T V^* (Q^* + E_3^*) U) U^* (A_u + E_1) U \\
&\qquad \text{(using } W e_1 = e_1 \text{ and } e_{n+1}^T V^* = e_{n+1}^T \text{)} \\
&= \mp \| x \|_2 U^* (A_u + E_1)(B^* + E_4^*) e_1 e_{n+1}^T (Q^* + E_3^*)(A_u + E_1) U \\
&= U^* (\mp \| x \|_2 A_u B^* e_1 e_{n+1}^T Q^* A_u + E_5) U \\
&= U^* (A_r + E_5) U,
\end{aligned}$$

where

$$\| E_5 \|_2 \leq \| x \|_2 \left(2 \| E_1 \|_2 + \| E_3 \|_2 + \| E_4 \|_2 + \cdots \right). \tag{7.1}$$

The dots represent higher order terms. We now seek bounds on $\| E_3 \|_2$ and $\| E_4 \|_2$.

A transformation of the form $\hat{B} = W^* B U$ is effected entirely by turnovers that pass a rotator through the descending sequence of B rotators. A typical turnover has the form $B_i B_{i+1} U_i = \tilde{U}_{i+1} \tilde{B}_i \tilde{B}_{i+1}$. The new B sequence will contain $\tilde{B}_i \tilde{B}_{i+1}$. If we can show that the (forward) error in the computed $\tilde{B}_i \tilde{B}_{i+1}$ is a tiny quantity F_t, then that can be translated via unitary transformations to an equally tiny backward error E_t.

For clarification let us contrast the analysis of $A_u = QC^*B$ with that of B by itself. Each turnover is backward stable in the sense that there is a small backward error in the product of the three rotators. In A_u all three rotators resulting from the turnover remain in the matrix. By contrast, in B alone, two of the rotators remain in B and one is removed. We have not shown that there is a small backward error in each of the rotators, only in the product of the three.

Now let us take another look at the turnover. We begin with three rotators

$$\begin{bmatrix} c_1 & -s_1 & \\ s_1 & \overline{c}_1 & \\ & & 1 \end{bmatrix} \begin{bmatrix} 1 & & \\ & c_2 & -s_2 \\ & s_2 & \overline{c}_2 \end{bmatrix} \begin{bmatrix} c_3 & -s_3 & \\ s_3 & \overline{c}_3 & \\ & & 1 \end{bmatrix},$$

whose product is

$$\begin{bmatrix} c_1 c_3 - s_1 c_2 s_3 & -c_1 s_3 - s_1 c_2 \overline{c}_3 & s_1 s_2 \\ s_1 c_3 + \overline{c}_1 c_2 s_3 & -s_1 s_3 + \overline{c}_1 c_2 c_3 & -\overline{c}_1 s_2 \\ s_2 s_3 & s_2 c_3 & \overline{c}_2 \end{bmatrix}, \tag{7.2}$$

and we want to obtain three new rotators

$$\begin{bmatrix} 1 & & \\ & c_4 & -s_4 \\ & s_4 & \overline{c}_4 \end{bmatrix} \begin{bmatrix} c_5 & -s_5 & \\ s_5 & \overline{c}_5 & \\ & & 1 \end{bmatrix} \begin{bmatrix} 1 & & \\ & c_6 & -s_6 \\ & s_6 & \overline{c}_6 \end{bmatrix},$$

whose product is

$$\begin{bmatrix} c_5 & -s_5 c_6 & s_5 s_6 \\ c_4 s_5 & c_4 \overline{c}_5 c_6 - s_4 s_6 & -c_4 \overline{c}_5 s_6 - s_4 \overline{c}_6 \\ s_4 s_5 & s_4 \overline{c}_5 c_6 + \overline{c}_4 s_6 & -s_4 \overline{c}_5 s_6 + \overline{c}_4 \overline{c}_6 \end{bmatrix}. \tag{7.3}$$

Since (7.2) and (7.3) must be equal, we obtain immediately some relationships. For example, from the first column we get

$$c_5 = c_1 c_3 - s_1 c_2 s_3, \qquad c_4 s_5 = s_1 c_3 + \overline{c}_1 c_2 s_3, \qquad \text{and} \qquad s_4 s_5 = s_2 s_3.$$

If we do these computations, we can then obtain

$$s_5 = \sqrt{|\, c_4 s_5 \,|^2 + (s_4 s_5)^2},$$

after which we obtain c_4 and c_5 by division by s_5. Now looking at the first row we find that

$$s_5 c_6 = c_1 s_3 + s_1 c_2 \overline{c}_3 \qquad \text{and} \qquad s_5 s_6 = s_1 s_2,$$

from which we can obtain c_6 and s_6 by division by s_5. This completes the computation. There is an analogous reverse operation, doing the turnover in the opposite direction, which we do not bother to write down.

We do not recommend this as a practical way of computing a turnover, but it does expose the relationships between quantities. It shows that we must divide by s_5 (or s_2 if we are going in the other direction), and no matter how we compute the turnover in practice, we cannot avoid division by s_5. It also exposes the "conservation laws" $s_4 s_5 = s_2 s_3$ and $s_5 s_6 = s_1 s_2$ (which are also related to theorems like 4.1 and 4.5.)

When we do the computations, each operation produces a small relative error. Since none of the numbers involved have magnitude greater than one, these small relative errors are also small absolute errors. Consider, for example, the computation of c_4. First we compute the intermediate quantity $\alpha = (c_4 s_5) = s_1 c_3 + \overline{c}_1 c_2 s_3$. The computed value will satisfy $\mathrm{fl}(\alpha) = \alpha + \epsilon_1$, where $|\, \epsilon_1 \,|$ is no larger than a small multiple of the unit roundoff. Because of the possibility of cancellation in the computation, we cannot claim that the relative error is small. Similarly, when we compute s_5, we get $\mathrm{fl}(s_5) = s_5 + \epsilon_2$. Then

$$\mathrm{fl}(c_4) = \mathrm{fl}\left(\frac{\gamma}{s_5}\right) = \frac{\gamma + \epsilon_1}{s_5 + \epsilon_2}(1 + \epsilon_3),$$

where ϵ_3 is the rounding error from the division. Doing some simple algebra we obtain

$$\mathrm{fl}(c_4) = c_4 + \frac{\epsilon_1}{s_5}(1 + \epsilon_3 - \frac{\epsilon_2}{s_5} + \cdots),$$

where the dots signify higher order terms. Thus the absolute error in the computation is roughly ϵ_1 / s_5. We can guarantee that this is small if and only if we can guarantee that s_5 is not too small.

When we do the turnover computation in practice, we might or might not do the exact sequence of operations shown here, but in every case, each c_i and s_i will be computed by a short sequence of floating point operations involving at most one division by s_5. Therefore we can say that for each of the computed rotators there will be a forward error on the order of $u/|\, s_5 \,|$, where u is the unit roundoff. Thus $\mathrm{fl}\left(\tilde{B}\right) = \tilde{B} + F$, where $\|\, F \,\|_2$ is a modest multiple of $u/|\, s_5 \,|$.

Now let us return to the specific turnover of interest: $B_i B_{i+1} U_i = \tilde{U}_{i+1} \tilde{B}_i \tilde{B}_{i+1}$, which passes a rotator through the descending B sequence. Here the role of s_5 is played by the subdiagonal entry of $\tilde{B}_i$. Thus, using Theorem 4.5, $|\, s_5 \,| = \beta_i \geq \beta_1 \cdots \beta_n = |\, a_0 \,| / \|\, x \,\|_2$. Thus the forward error is no worse than a modest multiple of $u \|\, x \,\|_2 / |\, a_0 \,|$. This also holds for the entire transformation from B to $\hat{B}$, which is just a sequence of n such turnovers. The small forward error can be converted to a small backward error.

THEOREM 7.1. *$\hat{B} = W^*(B + E_4)U$, where $\|\, E_4 \,\|_2$ is on the order of $u \|\, x \,\|_2 / |\, a_0 \,|$.*

A similar result holds for the transformation of C to $\hat{C}$. This result uses Theorem 4.1 instead of 4.5 and is better because it does not include the factor $|a_0|$.

THEOREM 7.2. *$\hat{C} = W^*(C + E_6)V$, where $\|E_6\|_2$ is on the order of $u\|x\|_2$.*

Finally, with a bit more work, we get a backward error result for the transformation from Q to $\hat{Q}$.

THEOREM 7.3. *$\hat{Q} = U^*(Q + E_3)V$, where $\|E_3\|_2$ is on the order of $u\|x\|_2/\gamma$, $\gamma = \min\{1, |a_0|\}$.*

Proof. $\hat{Q} = (\hat{Q}\hat{C}^*\hat{B})\hat{B}^*\hat{C} = \hat{A}_u\hat{B}^*\hat{C} = U(A_u + E_1)(B^* + E_4^*)(C + E_6)V = U^*(A_uB^*C + E_3)V = U^*(Q + E_3)V$, where $E_3 = E_1 + E_4^* + E_6 + \cdots$. Thus, to first order, $\|E_3\|_2 \le \|E_1\|_2 + \|E_4\|_2 + \|E_6\|_2$. The result follows. □

If we now refer back to (7.1), we can see that the rank-one part of our matrix satisfies $\hat{A}_r = U^*(A_r + E_5)U$, where $\|E_5\|_2$ is on the order of $u\|x\|_2^2/\gamma$, $\gamma = \min\{1, |a_0|\}$. We can now combine the unitary and rank-one parts to get our final result. Note that $1 \le \|x\|_2 \le \|A\|_2$, and in fact $\|x\|_2 \approx \|A\|_2$.

THEOREM 7.4. *Let $\hat{A}$ be the result of one step of our algorithm, starting from A. Let $\gamma = \min\{1, |a_0|\}$, and let u denote the unit roundoff. Then $\hat{A} = U^*(A + E)U$, where $\|E\|_2$ is on the order of $u\|A\|_2^2/\gamma$.*

7.1. Discussion. Our analysis shows that if the coefficients of the polynomial are not too large and $|a_0|$ is not too small, we get an excellent backward error. The two weaknesses of the analysis are that the square of $\|A\|_2$ appears in the bound and the factor $|a_0|$ appears in the denominator.

The square of the norm. It is expected that the bound would contain $\|A\|_2$ but disappointing that it contains a square. The extra factor suggests that the backward error of our method should deteriorate as $\|A\|_2$ increases, but we have not seen this in practice. The new method typically remains about as accurate as the unstructured Francis QR method, for which the backward error contains only a single factor $\|A\|_2$.

In our method the second factor $\|A\|_2$ appears in the analysis because we make estimates like $\beta_i \ge \beta_1 \cdots \beta_n = |a_0|/\|x\|_2$ from Theorem 4.5 and $\gamma_i \ge \gamma_1 \cdots \gamma_n = 1/\|x\|_2$ from Theorem 4.1. Typically we expect each γ_i to be much larger than the product $\gamma_1 \cdots \gamma_n$, so $1/\|x\|_2$ will normally be an extreme underestimate of all γ_i.

The factor $|a_0|$. The analysis suggests that the method might suffer instability in cases when $|a_0|$ is extremely small. One remedy for this would be to shift the basis and compute a new set of coefficients for which $|a_0|$ is not small. This can be done with cn^2 work where c is a small constant. We have not pursued this option, as our numerical experience suggests that a small value of a_0 does not normally result in instability. The factor a_0 shows up because of the estimate $\beta_i \ge \beta_1 \cdots \beta_n = |a_0|/\|x\|_2$ from Theorem 4.5. Again we note that this is likely to be an extreme underestimate. Notice, moreover, that in the initial configuration we have $B_i = C_i$, $i = 1, \ldots, n-1$, so the β_i are not small initially, except possibly β_n. In the extreme case $a_0 = 0$ we get $\beta_n = 0$, i.e. B_n is trivial. The smallness of β_n can be transmitted to the other β_i only slowly, and there are reasons to believe that the smallness will remain confined mainly to β_n. The small a_0 normally signals a root close to zero (especially if a_1 is not small). This tiny eigenvalue will be found and deflated out in a few iterations. After the first deflation B_n ceases to participate in subsequent iterations. If the smallness is trapped there, it will not do any harm. In fact equation (4.10) implies that the deflated eigenvalue λ satisfies $|\lambda| = \beta_n/\gamma_n$, so if λ is tiny, then β_n must also be tiny. This means that the smallness stays in B_n. Notice also that B_n never plays the role of the central rotator (the one containing s_5) in the turnover. Thus, if the smallness

Deg.	No. runs	Deg.	No. runs	Deg.	No. runs	Deg.	No. runs
6	16384	14	2048	128	128	2048	8
8	16384	16	1024	256	64	4096	4
10	8192	32	512	512	32	8192	2
12	4096	64	256	1024	16	16384	1

Table 8.1: Number of runs for each polynomial degree considered.

remains in B_n, it will never do any damage.

Remark 7.5. One could consider a variant of our algorithm in which y is stored and updated explicitly. Any information about the rank-one part that is needed would be drawn from this explicitly stored y instead of the B and C rotators. For this algorithm one can easily prove the backward stability of the rank-one part, obtaining a backward error expression containing $\|A\|_2$ *only, not the square. Unfortunately this variant does not work at all well. Over the course of iterations, roundoff errors will cause the explicitly stored y to disagree more and more with the implicitly defined y given by the rotators. As a consequence R and A will cease to be upper triangular and upper Hessenberg, respectively, and the algorithm will perform poorly.*

8. Numerical experiments. Speed and accuracy of both the single and double shift implementation (AMVW) are examined and compared with other companion QR algorithms: LAPACK's Hessenberg eigenvalue solver (xHSEQR), LAPACK's eigensolver for general matrices (xGEEV)[2], which balances the problem first, the method of Boito, Eidelman, Gemignani, and Gohberg [11] (BEGG) and the algorithm of Chandrasekaran, Gu, Xia, and Zhu [13] (CGXZ). BEGG only has a single shift implementation and CGXZ is only available as a double shifted version.

We also experimented with the codes of Bini, Boito, Eidelman, Gemignani, and Gohberg [5], available in both single shift and double shift versions. We found that their single shift code was slightly slower than BEGG, and their double shift code was marginally faster than CGXZ. These codes were, however, often much less accurate than the others. Therefore, we did not included the results from these codes.

The computations were executed on an Intel Core i5-3570 CPU running at 3.40 GHz with 8GB of memory. GFortran 4.6.3 was used to compile the Fortran codes.

We have data from four categories of experiments: polynomials with random coefficients, polynomials with roots of unity of the form $z^n - 1$, special polynomials used for testing polynomial solvers [8, 13, 22, 26], and polynomials designed to test the stability of the code. In the first two experiments, see Sections 8.1 and 8.2, the computing time was examined. The depicted runtime is averaged over a decreasing number of runs, as shown in Table 8.1. The accuracy is investigated in all experiments, with the error measure adapted to the type of experiment and described further on.

8.1. Polynomials with random coefficients. Polynomials with random coefficients in the monomial basis are known to be well-conditioned as their eigenvalues are typically located around the unit circle. The coefficients are normally distributed with mean 0 and variance 1. For testing the single shift code complex coefficients were used, while real polynomials were piped to the double shift code.

[2] xHSEQR and xGEEV are either the complex implementations ZHSEQR and ZGEEV or the real double precision ones DHSEQR and DGEEV.

The measure of accuracy for a single problem size is the maximum of all relative residuals of all computed eigenpairs over 10 runs, where the relative residual for a particular eigenpair (λ, v) equals

$$\frac{\|Av - \lambda v\|_\infty}{\|A\|_\infty \|v\|_\infty}. \tag{8.1}$$

For avoiding over-, underflow, and easily computing the eigenvectors we refer to [2].

Figures 8.1 and 8.2 illustrate that the accuracy of AMVW is comparable to that of LAPACK, significantly better than BEGG, and slightly better than CGXZ. Considering speed, we note that we are more than three times faster than BEGG in the single shift case, and we become faster than LAPACK for polynomials of degree 12 or greater. In the double shift case the speed up is less pronounced, but the AMVW time is still less than half that of CGXZ. The crossover with LAPACK now takes place at degree 16.

Jenkins and Traub [22] state that polynomials with normally distributed random coefficients are a "poor choice as the randomness 'averages out' in the coefficients and the polynomials differ but little from each other". Therefore we also used the test set (iv) from [22], polynomials with random coefficients $a_j = m_j \cdot 10^{e_j}$, having m_j uniformly distributed in $(-1, 1)$ and e_j uniformly distributed in $(-\mu, \mu)$, with $\mu = 5, 10, 15, 20, 25$. The results were very similar to those for normally distributed coefficients, so we have not displayed them.

8.2. Polynomials $z^n - 1$. The polynomials with roots of unity $z^n - 1$ also have well-conditioned roots as the companion matrix itself is unitary. Furthermore, the roots lie on the unit-circle and are known exactly: $z_j = \cos(\frac{2j}{n}\pi) + i \cdot \sin(\frac{2j}{n}\pi)$, $j = 0, \ldots, n-1$, where i is the imaginary unit. The accuracy here is the maximum absolute difference between the computed and the exact roots, which also equals the maximum relative difference.

The results shown in Figures 8.3 and 8.4 are along the same lines as for the random case. In the single shift case our accuracy is comparable to that of LAPACK and better than BEGG. For the double shift case, we perform slightly better than the other approaches. In the single shift case, we are more than three times faster than the fastest currently available approach, in the double shift case, twice as fast.

8.3. Special real polynomials. In this section we have computed roots of difficult polynomials and reported the forward and backward error of the various methods. All of the test polynomials have real coefficients and we used them to test both the real and the complex codes. In cases where the roots are known either exactly or to high accuracy, we report the maximum relative forward error. To get a measure of backward error, we take the computed roots and use extended precision arithmetic to compute the coefficients $\hat{a}_i$ of a polynomial having those roots. We then compare these to the original a_i. To compute the $\hat{a}_i$ we used the multiprecision arithmetic from [25] and a function from the CGXZ code [13]. The backward error measure is the maximal error on the coefficients relative to the norm of the coefficients

$$\max_i \frac{|a_i - \hat{a}_i|}{\|x\|_2}, \tag{8.2}$$

with $x = -[a_1, \ldots, a_{n-1}, a_0, 1]$.

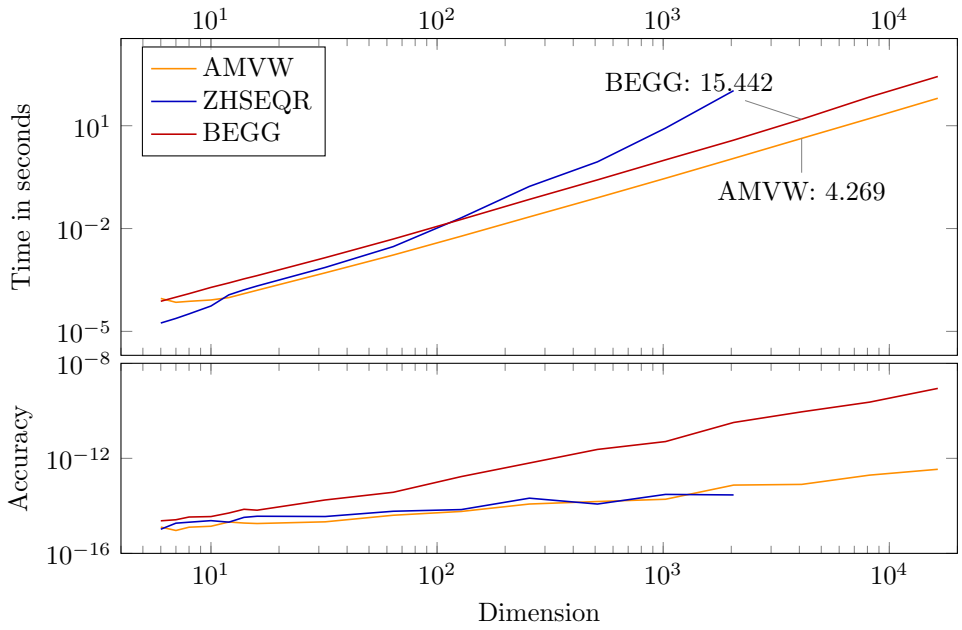

Fig. 8.1: Runtime and accuracy for the single shift code for random coefficients.

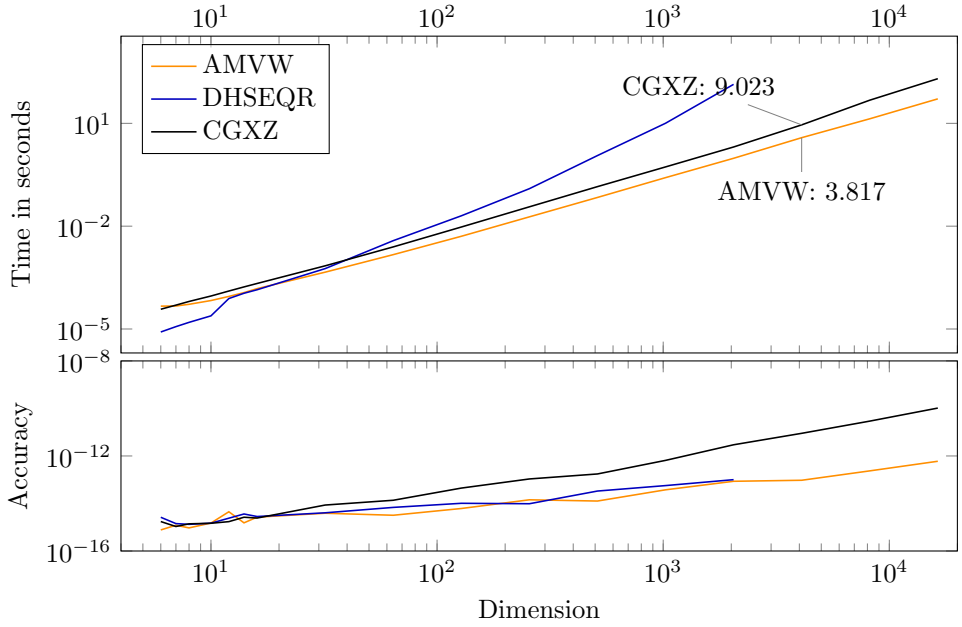

Fig. 8.2: Runtime and accuracy for the double shift code for random coefficients.

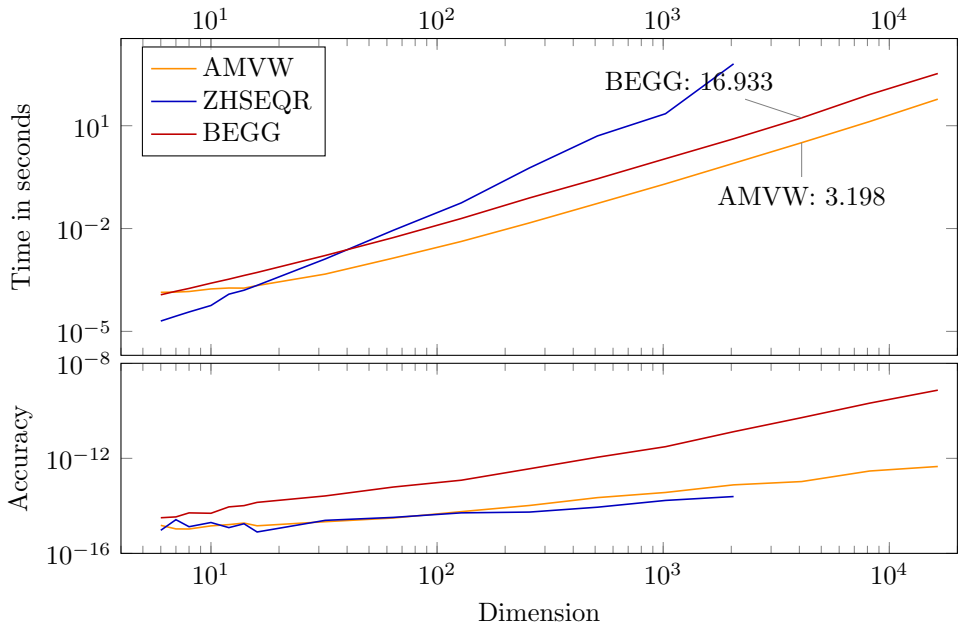

Fig. 8.3: Runtime and accuracy for the single shift code for roots of unity.

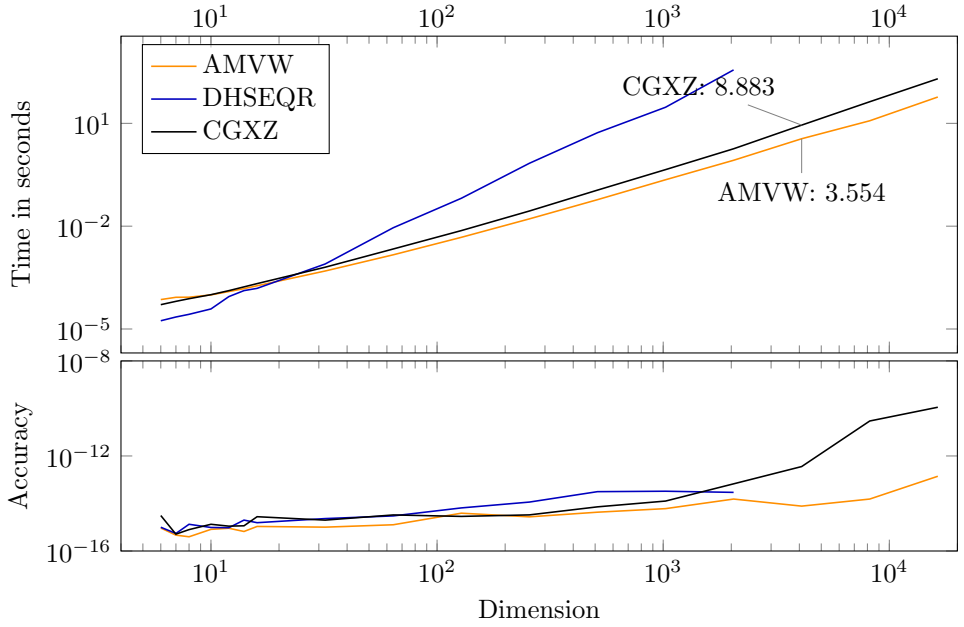

Fig. 8.4: Runtime and accuracy for the double shift code for roots of unity.

Balancing. The LAPACK codes that we have used in these tests are xHSEQR, which does not balance, and xGEEV, which has a balancing step. As the tables below show, balancing is occasionally very helpful, but there are also examples where balancing is detrimental.

As our algorithm relies on the unitary-plus-rank-one structure of the companion matrix, we do not have as much freedom to balance as one has in general. In particular, the diagonal balancing strategy used by xGEEV is not available. However, we do have the freedom to replace $p(z)$ by $\alpha^{-n}p(\alpha z)$, where α is a positive scalar chosen to even out the coefficients of the polynomial. An efficient and reliable strategy for choosing α is not known; this is a question that requires further study. We have just implemented one very simple strategy here: We chose α so that the magnitude of the constant term is 1. All solvers were tested on both the original polynomials and on polynomials balanced in this way. The results for the balanced polynomials were reported only in those cases where there was a significant difference between results for the balanced and unbalanced polynomials. In some cases balancing was beneficial, but in other cases it was harmful.

The test set. The first 11 polynomials, Table 8.2, are polynomials also tested in [13], for which the roots are known: Wilkinson polynomials and polynomials with particular distributions of the roots. As part of the investigations we added polynomial 9 as it triggers a special behavior of the CGXZ code compared to polynomial 8.

No.	Description	Deg.	Roots
1	Wilkinson polynomial	10	$1, \ldots, 10$
2	Wilkinson polynomial	15	$1, \ldots, 15$
3	Wilkinson polynomial	20	$1, \ldots, 20$
4	scaled and shifted Wilkinson poly.	20	$-2.1, -1.9, \ldots, 1.7$
5	reverse Wilkinson polynomial	10	$1, 1/2, \ldots, 1/10$
6	reverse Wilkinson polynomial	15	$1, 1/2, \ldots, 1/15$
7	reverse Wilkinson polynomial	20	$1, 1/2, \ldots, 1/20$
8	prescribed roots of varying scale	20	$2^{-10}, 2^{-9}, \ldots, 2^{9}$
9	prescribed roots of varying scale -3	20	$2^{-10} - 3, \ldots, 2^{9} - 3$
10	Chebyshev polynomial	20	$\cos(\frac{2j-1}{40}\pi)$
11	$z^{20} + z^{19} + \cdots + z + 1$	20	$\cos(\frac{2j}{21}\pi)$

Table 8.2: Special polynomials tested by Chandrasekaran et al. in [13].

Some polynomials taken from MPSolve [8] are given in Table 8.3. We assume the roots computed by MPSolve, using variable precision arithmetic, to be exact. The MPSolve collection contains many polynomials deliberately designed to be too ill conditioned to solve in double precision arithmetic; we did not report on those. In [8] it is stated that the polynomial trv_m, provided by Carlo Traverso, arises from the symbolic processing of a system of polynomial equations and has multiple roots. The Mandelbrot polynomials are defined iteratively as follows $p_0(z) = 1$, $p_i(z) = zp_{i-1}(z)^2 + 1$, for $i = 1, 2, \ldots, k$, with $n = 2^k - 1$.

The examples in Table 8.4, were created for us by Vanni Noferini. The polynomials have normal distributed real roots with mean 0 and standard deviation 1, where one random root is scaled by 1 e+12 and another one by 1 e+9. These polynomials are difficult to balance.

No.	Description	Deg.	Roots
12	trv_m, C. Traverso	24	known
13	mand31 Mandelbrot example ($k = 5$)	31	known
14	mand63 Mandelbrot example ($k = 6$)	63	known

Table 8.3: Special polynomials used to test MPSolve in [8].

No.	Description	Deg.	Roots
15	polynomial from V. Noferini	12	almost random
16	polynomial from V. Noferini	35	almost random

Table 8.4: Special polynomials provided by V. Noferini.

The polynomials in Table 8.5 stem from [22] and were designed to test particular properties of rootsolvers. The cubic polynomial $p_1(z) = (z-a)(z+a)(z-1)$, used in test cases $17-20$ examines the termination criteria, i.e. convergence difficulties; $p_3(z) = \prod_{i=1}^{n}(z-10^i)$ checks the occurence of underflow; and $p_{10}(z) = (z-a)(z-1)(z-a^{-1})$ and $p_{11}(z) = \prod_{k=1-m}^{m-1}\left(z-\exp\left(\frac{ik\pi}{2m}\right)\right)\prod_{k=m}^{3m}\left(z-0.9\exp\left(\frac{ik\pi}{2m}\right)\right)$ having zeros on two half-circles examine the deflation strategy.

No.	Description	Deg.	Roots
17	$p_1(z)$ with $a =$1 e−8	3	1 e−8, -1 e−8, 1
18	$p_1(z)$ with $a =$1 e−15	3	1 e−15, -1 e−15, 1
19	$p_1(z)$ with $a =$1 e+8	3	1 e+8, -1 e+8, 1
20	$p_1(z)$ with $a =$1 e+15	3	1 e+15, -1 e+15, 1
21	$p_3(z)$ underflow test	10	1 e−1, . . . ,1 e−10
22	$p_3(z)$ underflow test	20	1 e−1, . . . ,1 e−20
23	$p_{10}(z)$ deflation test $a =$ 10 e+3	3	1, 1 e+3, 1 e−3
24	$p_{10}(z)$ deflation test $a =$ 10 e+6	3	1, 1 e+6, 1 e−6
25	$p_{10}(z)$ deflation test $a =$ 10 e+9	3	1, 1 e+9, 1 e−9
26	$p_{11}(z)$ deflation test $m = 15$	60	$\exp(\frac{ik\pi}{2m})$, $0.9\exp(\frac{ik\pi}{2m})$

Table 8.5: Polynomials to test root finding algorithms from [22].

Table 8.6 reports the Bernoulli polynomial $\sum_{k=0}^{n}\binom{n}{k}b_{n-k}z^k$, with the Bernoulli numbers of the first kind b_{n-k}, and the truncated exponential $k!\sum_{k=0}^{n}\frac{z^k}{k!}$.

No.	Description	Deg.	Roots
27	Bernoulli polynomial ($k = 20$)	20	—
28	truncated exponential ($k = 20$)	20	—

Table 8.6: Bernoulli and truncated exponential.

The polynomials in Table 8.7 were used in [4] and originate from [1, 9, 12]:

$$p_1(z) = 1 + \left(\frac{m}{m+1} + \frac{m+1}{m}\right) z^m + z^{2m},$$
$$p_2(z) = \frac{1}{m}\left(\sum_{j=0}^{m-1}(m+j)z^j + (m+1)z^m + \sum_{j=0}^{m-1}(m+j)z^{2m-j}\right),$$
$$p_3(z) = (1-\lambda)z^{m+1} - (\lambda+1)z^m + (\lambda+1)z - (1-\lambda).$$

These polynomials exhibit particular symmetries, with $p_1(z)$ and $p_2(z)$ palindromic and $p_3(z)$ anti-palindromic.

No.	Description	Deg.	Roots
29–33	$p_1(z)$ with $m = 10, 20, 30, 256, 512$	$2m$	—
34–38	$p_2(z)$ with $m = 10, 20, 30, 256, 512$	$2m$	—
39–43	$p_3(z)$ with $m+1 = 20, \ldots, 1024$, $\lambda = 0.9$	$m+1$	—
44–48	$p_3(z)$ with $m+1 = 20, \ldots, 1024$, $\lambda = 0.999$	$m+1$	—

Table 8.7: Polynomials tested in [4], coming from [1, 9, 12].

Discussion. For the single and double shift codes, forward and backward errors of both balanced and unbalanced polynomials are reported. Note, however, that the results of the unbalanced polynomials are shown only for those cases where balancing had a significant impact. To make a fair comparison with an unstructured QR algorithm on the companion matrix we added to each table a column containing the results linked to xGEEV, allowing for a more advanced balancing. This also implies that the results of xGEEV in Tables 8.9, 8.11, 8.13, and 8.15 originate from a balanced polynomial, put in a companion matrix balanced once more before its roots were computed.

Tables 8.8 and 8.9 depict the results for the single shifted code, without and with balancing, respectively. Comparing first LAPACK's balanced (ZGEEV) and unbalanced (ZHSEQR) solver we see that in general the additional scaling does improve the forward error, as seen in polynomials 5, 6, 8, 12, and 17-22. Only V. Noferini's polynomials 15 and 16 seem to suffer from the balancing. We can deduce that almost always the forward error of AMVW is in the close proximity of the one of LAPACK's ZHSEQR; except for the polynomials 3, 12, 17, 18, and 21, but balancing those polynomials brings the forward error up to the same level as ZHSEQR, sometimes even better as illustrated by polynomials 17 and 18. For polynomial 8, however, we seem to be unable to achieve the accuracy of the full balanced ZGEEV method. One should be careful with balancing, however, e.g., for polynomial 20 AMVW loses 5 decimal places w.r.t. the unbalanced version, whereas BEGG gains 8; also for polynomials 15 and 16 the balancing is disastrous.

Tables 8.10 and 8.11 report the backward errors for the single shifted code, without and with balancing, respectively. Overall we can state by looking at Table 8.10 that the backward error is almost always at the level of machine precision, and comparable to the error of LAPACK's ZHSEQR and ZGEEV. Moreover, we have an excellent backward error for polynomials 15 and 16, whereas ZGEEV looses quite some digits;

No.	AMVW	ZHSEQR	ZGEEV	BEGG
1	2.1050 e−10	2.2132 e−11	1.8227 e−10	2.6921 e−11
2	5.0840 e−06	1.9949 e−06	2.9499 e−06	6.2327 e−08
3	6.4836 e+00	4.7536 e−03	3.0706 e−03	9.9687 e−01
4	3.4537 e−12	9.9365 e−13	9.6145 e−13	8.2891 e−13
5	2.9382 e−06	3.8860 e−06	8.2346 e−10	4.3172 e−06
6	4.3553 e−01	4.7760 e−01	1.0849 e−04	5.1168 e−01
7	2.1438 e+00	2.4780 e+00	2.7442 e−01	2.2530 e+00
8	3.3777 e−01	1.5862 e+00	2.8288 e−13	1.0000 e+00
9	6.6578 e−02	3.5919 e−02	4.7317 e−02	8.8937 e−01
10	1.2156 e−10	3.6616 e−11	5.3622 e−12	2.6118 e−11
11	1.5779 e−15	3.0227 e−15	2.2861 e−15	1.3545 e−14
12	1.1470 e+02	2.3742 e−04	7.0187 e−08	2.0689 e−04
13	1.2361 e−06	5.9051 e−06	1.0481 e−06	2.9379 e−07
14	2.3801 e−01	2.3893 e−01	2.1137 e−01	1.8421 e−01
15	6.2579 e−13	4.1005 e−13	6.4643 e−09	4.5861 e+00
16	3.1063 e−04	1.5007 e−04	7.6375 e−02	9.5143 e+00
17	5.3671 e−02	6.4531 e−09	2.2830 e−14	1.0000 e+00
18	5.2684 e+06	4.5303 e−02	1.5777 e−15	1.0000 e+00
19	5.0000 e−09	4.5648 e−01	4.4703 e−16	1.2872 e−01
20	7.5000 e−16	7.0539 e+06	1.2500 e−16	2.5385 e+13
21	1.8865 e+07	1.0000 e+00	3.2526 e−15	9.1219 e+07
22	2.8557 e+16	9.7471 e+15	1.2585 e−13	1.5085 e+17
23	4.0658 e−16	2.2204 e−16	1.3323 e−15	2.1103 e−12
24	5.2940 e−16	3.7253 e−16	4.4409 e−16	5.2636 e−10
25	1.2925 e−16	1.1102 e−15	7.7716 e−16	1.7481 e−06
26	3.9438 e−08	6.8424 e−08	1.5569 e−08	3.3993 e−08

Table 8.8: Unbalanced single shift version: relative forward errors.

No.	AMVW	ZHSEQR	ZGEEV	BEGG
3	1.0936 e−02	1.6164 e−02	1.3548 e−02	3.0069 e−03
5	1.3543 e−09	3.3472 e−10	1.9049 e−10	1.7691 e−10
6	2.4207 e−06	4.6529 e−05	6.5809 e−07	4.8093 e−07
7	7.3168 e−02	7.8505 e−02	3.5468 e−02	9.3801 e−04
8	2.6127 e−03	1.0478 e−01	1.0003 e−13	4.2559 e+00
12	9.4884 e−08	6.5912 e−08	6.5913 e−08	6.5914 e−08
15	1.7688 e−08	1.6919 e−01	3.7136 e−08	1.4816 e+01
16	4.0845 e+00	2.3640 e+00	2.8642 e−01	5.5635 e+00
17	3.3307 e−16	8.0898 e−14	8.0898 e−14	1.9533 e−12
18	2.2204 e−16	1.3331 e−11	1.3331 e−11	7.8722 e−08
19	5.8531 e−13	2.4438 e−14	7.4506 e−16	6.7711 e−13
20	5.0957 e−11	3.7500 e−16	2.5000 e−16	2.0993 e−08
21	1.7896 e−08	6.7911 e−09	4.1200 e−15	1.8439 e−07

Table 8.9: Balanced single shift version: relative forward errors.

No.	AMVW	ZHSEQR	ZGEEV	BEGG
1	5.1196 e−15	4.1115 e−16	5.8997 e−16	1.5451 e−15
2	3.9604 e−15	1.3259 e−15	8.2223 e−15	3.4513 e−15
3	1.0444 e−14	4.4686 e−15	1.0897 e−14	3.3521 e−01
4	2.5540 e−15	1.4871 e−15	4.7586 e−15	1.4956 e−14
5	8.2139 e−16	1.0871 e−15	1.3384 e−15	2.1723 e−15
6	2.2860 e−15	2.5367 e−15	1.0886 e−15	1.2435 e−14
7	2.2331 e−15	1.2368 e−15	1.2356 e−15	2.9261 e−14
8	2.7015 e−15	4.4440 e−16	4.4440 e−15	4.3155 e−14
9	2.7186 e−14	4.3771 e−15	1.7130 e−15	5.4169 e−01
10	1.5407 e−15	2.5169 e−15	2.8764 e−15	1.7898 e−14
11	2.0003 e−15	2.8510 e−15	3.5121 e−15	2.6659 e−14
12	4.7822 e−15	9.4479 e−13	4.7233 e−15	4.7723 e−06
13	4.9819 e−15	4.3757 e−15	2.7359 e−15	2.2766 e−14
14	1.8597 e−15	3.8582 e−15	6.5575 e−15	5.5561 e−14
15	1.3389 e−15	2.1200 e−15	2.7315 e−12	7.5294 e−01
16	3.3954 e−15	1.2577 e−15	1.7363 e−10	4.8497 e−01
17	7.0711 e−17	2.3551 e−16	3.1702 e−22	8.6299 e−17
18	1.9626 e−17	4.7103 e−16	1.2551 e−30	1.5701 e−16
19	2.8284 e−16	7.9289 e−01	5.2684 e−24	1.7032 e−01
20	9.9516 e−17	3.5184 e+13	9.9516 e−17	7.0711 e−01
21	6.8952 e−16	8.8275 e−16	1.2931 e−18	7.6787 e−15
22	4.2578 e−16	1.2713 e−15	4.1379 e−17	1.0589 e−13
23	2.5722 e−16	3.8583 e−16	1.4147 e−15	5.1444 e−16
24	1.3171 e−16	2.6342 e−16	5.2684 e−16	6.8489 e−15
25	1.5701 e−26	8.0922 e−16	5.3948 e−16	7.0711 e−11
26	7.6615 e−15	8.8366 e−15	1.0720 e−14	2.0853 e−13
27	2.1675 e−15	4.5595 e−15	1.7593 e−15	1.7038 e−14
28	3.1876 e−12	5.0699 e−14	3.2455 e−15	7.3074 e−03
29	4.9669 e−15	5.1055 e−15	3.7699 e−15	2.8623 e−14
30	9.5901 e−15	8.2199 e−15	1.1074 e−14	1.8039 e−13
31	9.9974 e−15	1.0205 e−14	1.5443 e−14	4.3526 e−13
32	2.1807 e−13	1.3192 e−13	1.7909 e−13	3.7859 e−11
33	8.0583 e−13	4.4225 e−13	2.3127 e−13	1.6207 e−10
34	2.9405 e−15	4.8468 e−15	2.5078 e−15	1.9583 e−14
35	4.9934 e−15	6.1108 e−15	8.8445 e−15	3.9206 e−14
36	6.4280 e−15	1.1107 e−14	9.6821 e−15	9.2465 e−14
37	7.1336 e−14	7.0023 e−14	2.9302 e−14	3.3525 e−12
38	8.0993 e−14	2.5129 e−13	7.2148 e−14	1.2479 e−11
39	3.0150 e−15	8.8480 e−15	5.3923 e−15	7.8171 e−14
40	4.8915 e−15	1.0332 e−14	1.0953 e−14	2.4283 e−13
41	8.9851 e−15	1.6620 e−14	2.8066 e−14	5.7554 e−13
42	2.5584 e−13	1.2546 e−13	3.1821 e−13	7.4880 e−11
43	3.4998 e−13	5.1111 e−13	3.6126 e−13	4.1188 e−10
44	2.6053 e−15	4.2770 e−14	1.4583 e−14	1.3910 e−13
45	5.8822 e−15	4.2237 e−14	1.7358 e−14	2.3743 e−13
46	8.0065 e−15	4.8979 e−14	1.7963 e−14	5.7847 e−13
47	4.2851 e−13	2.9020 e−13	4.7464 e−13	7.4323 e−11
48	1.9136 e−12	1.2078 e−12	9.1693 e−13	4.1296 e−10

Table 8.10: Unbalanced single shift version: backward error measure (8.2).

No.	AMVW	ZHSEQR	ZGEEV	BEGG
3	3.6523 e−12	9.3948 e−12	3.6005 e−15	4.0993 e−14
8	1.3945 e−15	4.3632 e−15	3.5552 e−15	8.0150 e−02
9	3.4155 e−11	1.8478 e−11	5.3243 e−15	3.3980 e−14
12	2.9828 e−14	7.8137 e−13	8.0198 e−15	5.1514 e−14
15	3.2535 e−12	3.5266 e−06	7.7020 e−11	1.8265 e+06
16	4.6922 e−04	9.1242 e−05	3.3598 e−09	4.4007 e+01
19	4.1352 e−13	1.4142 e−16	5.6569 e−16	9.3791 e−13
20	3.6032 e−11	1.9903 e−16	2.9855 e−16	2.9680 e−08
28	2.1364 e−14	1.3348 e−14	4.7639 e−15	4.6575 e−14

Table 8.11: Balanced single shift version: backward error measure (8.2).

and for polynomials 19 and 20 we perform very well, whereas ZHSEQR fails completely; only for polynomial 28 we are 2-3 digits behind. Polynomial 28 is the only case where balancing seems to help AMVW, for all other cases the balancing has no or a negative effect on the backward error, e.g., we record a dramatic loss for polynomial 16. Also for the backward error, the effect of the balancing strongly depends on the method, e.g., ZHSEQR behaves dissimilar in cases 10 and 19 compared to 15 and 16.

Tables 8.12 and 8.13 report the data of the double shift code with and without balancing. The forward errors of all three methods, excluding DGEEV, are typically comparable, except for polynomials 8, 12, and 18 we are worse than CXGZ, and for 12 also much worse than DHSEQR. Except for polynomials 15 and 16, DGEEV provides the best forward error. After balancing we achieve an error comparable to the one of CXGZ for 12 and 18, but not for polynomial 8. Polynomial 8 is an interesting case. The representation of CXGZ and the fact that it operates on a row companion matrix[3] seems to make CXGZ particularly suited to solve this polynomial with excellent forward error. The backward error, however, of all methods is excellent as shown in Table 8.14. But, if one shifts the roots by -3 as done deliberately by us in polynomial 9, CXGZ loses its advantages.

Tables 8.14 and 8.15 depict the backward errors for the double shift code. The most interesting polynomials, when comparing AMVW with LAPACK, are 12, 15-16, 18-20, otherwise we are in each other's proximity. AMVW appears quite robust for the balancing; we gain accuracy in cases 12, 19, and 20 and arrive at the same level as LAPACK, but we lose accuracy for polynomials 3, 9, 15, and 16. CXGZ, on the other hand seems to benifit often from the balancing, e.g., cases 1, 2, and 3.

8.4. Additional Backward Stability Tests. The backward stability analysis (Theorem 7.4) suggests that if the polynomial coefficients are large (i.e. $\|x\|_2$ and $\|A\|_2$ are large) or $|a_0|$ is small, stability problems might occur. In fact we have not observed this in practice. Here we present two typical experiments. In the first we use random coefficients scaled so that $\|a\|_2$ takes on successively larger values, where $a = \begin{bmatrix} a_0 & \cdots & a_{n-1} \end{bmatrix}$. (As always, $a_n = 1$.) Our measure of backward error is the relative residual (8.1). We see from Table 8.16 that increasing $\|a\|_2$ does not decrease backward stability. There is no evidence of any influence of $\|a\|_2^2$.

[3]This triggers initial zero shifts, as a consequence the smallest roots are computed first up to high accuracy.

No.	AMVW	DHSEQR	DGEEV	CGXZ
1	1.6210 e−10	4.9825 e−11	2.3028 e−10	1.5539 e−09
2	1.3451 e−05	2.0112 e−06	2.8902 e−06	4.0939 e−02
3	1.1105 e−01	4.7901 e−03	1.9342 e−03	1.1366 e+00
4	1.0592 e−11	9.7908 e−13	9.6026 e−13	1.3891 e−12
5	2.9139 e−06	7.3219 e−07	4.6375 e−09	5.2079 e−07
6	3.1037 e−01	4.7761 e−01	1.0670 e−04	2.7667 e−01
7	2.1373 e+00	2.4780 e+00	2.7437 e−01	1.7181 e+00
8	1.3517 e−02	1.5862 e+00	2.9221 e−13	2.3874 e−12
9	6.9255 e−02	3.6109 e−02	4.7155 e−02	3.6172 e−02
10	9.1321 e−11	3.5446 e−11	2.7766 e−12	8.4860 e−12
11	2.1897 e−15	1.7772 e−15	1.7902 e−15	1.5029 e−15
12	3.8450 e+09	1.5396 e−07	6.5915 e−08	9.9998 e−01
13	1.6734 e−06	5.8771 e−06	1.4481 e−06	1.2551 e−07
14	1.9244 e−01	2.3890 e−01	2.0926 e−01	1.8676 e−01
15	3.5791 e−13	2.8406 e−13	1.6215 e−07	6.5713 e−09
16	5.0829 e−02	6.0853 e−02	3.4274 e−01	3.1499 e−02
17	1.5574 e−01	1.5467 e−01	1.6544 e−16	4.9644 e−01
18	2.3283 e+05	1.1886 e+07	0.0000 e+00	1.0000 e+00
19	3.4217 e−02	0.0000 e+00	2.2204 e−16	2.9289 e−01
20	1.4074 e+14	1.1102 e−16	2.5000 e−16	8.9582 e+13
21	8.2155 e+06	8.3282 e+05	3.3881 e−15	2.2859 e+04
22	1.3689 e+17	1.2372 e+16	2.1125 e−13	3.9170 e+16
23	2.2204 e−16	2.7105 e−16	5.4570 e−16	1.1018 e−13
24	6.6310 e−14	1.3136 e−11	4.6322 e−15	4.9989 e−08
25	3.8147 e−16	1.8274 e−09	2.4169 e−14	5.0000 e−01
26	2.0278 e−08	6.9016 e−08	2.0442 e−08	2.0860 e−08

Table 8.12: Unbalanced double shift version: relative forward errors.

No.	AMVW	DHSEQR	DGEEV	CGXZ
2	2.5408 e−07	6.4221 e−07	1.4197 e−06	3.7187 e−08
3	4.3991 e−03	1.6125 e−02	1.3044 e−02	9.9774 e−05
5	1.1167 e−09	9.9303 e−10	7.7720 e−10	1.9518 e−10
6	9.5742 e−06	4.7094 e−05	4.6864 e−07	3.8280 e−07
7	9.1226 e−02	7.8035 e−02	3.6341 e−02	3.7364 e−03
12	1.2993 e−07	6.5912 e−08	6.5913 e−08	6.5913 e−08
15	2.8718 e−08	1.4421 e+00	1.3549 e−06	3.0468 e−11
16	9.3849 e+00	1.0386 e+00	3.0570 e−01	1.0000 e+00
17	1.4724 e−14	2.8245 e−12	2.8245 e−12	4.4409 e−16
18	2.3219 e−07	1.9722 e−16	1.9722 e−16	5.0000 e−06
19	5.9605 e−16	2.2204 e−16	2.2204 e−16	6.6613 e−16
20	1.1102 e−16	0.0000 e+00	2.2204 e−16	0.0000 e+00
21	4.6878 e−08	1.0450 e−04	4.3944 e−15	2.6235 e−11

Table 8.13: Balanced double shift version: relative forward errors.

No.	AMVW	DHSEQR	DGEEV	CGXZ
1	1.2554 e−15	3.5731 e−15	1.4486 e−15	1.5982 e−11
2	4.6694 e−15	2.4362 e−15	1.5226 e−15	1.8855 e−06
3	2.4299 e−14	4.9498 e−15	4.8598 e−15	1.6969 e−01
4	2.0819 e−15	4.7586 e−15	2.0394 e−15	2.6427 e−14
5	3.2376 e−16	4.1775 e−16	5.8485 e−16	4.5953 e−15
6	1.2676 e−15	1.2676 e−15	5.4327 e−16	1.6540 e−14
7	1.3531 e−15	1.2344 e−15	1.4243 e−15	1.8041 e−15
8	2.0200 e−15	4.1208 e−15	3.8784 e−15	2.3755 e−14
9	1.2532 e−15	3.0366 e−15	4.9163 e−15	1.7128 e−04
10	2.8916 e−15	3.2139 e−15	1.2145 e−15	2.1735 e−14
11	2.5681 e−15	4.1186 e−15	3.0526 e−15	1.9382 e−15
12	1.4556 e−06	4.7803 e−12	8.1089 e−15	9.9727 e−01
13	3.3535 e−15	2.0554 e−15	2.7044 e−16	1.0223 e−14
14	9.9463 e−15	5.3784 e−15	5.1942 e−15	2.7746 e−13
15	1.1921 e−15	1.8423 e−15	1.5479 e−10	5.5105 e−10
16	6.5917 e−15	2.6367 e−15	1.4353 e−10	2.3723 e−05
17	7.8505 e−17	1.8694 e−16	1.1698 e−24	2.3551 e−16
18	4.8682 e−18	9.9894 e−17	0.0000 e+00	3.1402 e−16
19	4.9218 e−02	0.0000 e+00	1.4142 e−16	3.5355 e−01
20	7.0711 e−01	9.9516 e−17	2.9855 e−16	7.1278 e−01
21	9.6550 e−17	8.8275 e−16	1.3793 e−17	1.1988 e−05
22	9.9309 e−16	8.0260 e−16	4.1379 e−17	9.8621 e−01
23	2.5722 e−16	1.2861 e−16	6.4305 e−16	3.8583 e−16
24	6.7435 e−14	2.6342 e−16	1.0537 e−15	3.5347 e−15
25	2.6974 e−16	1.3487 e−16	1.7036 e−24	3.5355 e−11
26	4.7127 e−15	1.0052 e−14	6.5066 e−15	1.9228 e−14
27	1.0238 e−15	1.9382 e−15	8.6142 e−15	6.6957 e−14
28	4.4046 e−14	4.3488 e−14	5.4360 e−15	6.8382 e−01
29	2.5594 e−15	2.8052 e−15	5.3901 e−15	5.4346 e−15
30	3.7532 e−15	1.2390 e−14	1.7220 e−14	2.9183 e−14
31	7.7228 e−15	1.2892 e−14	1.5818 e−14	1.9156 e−14
32	6.4705 e−14	9.7108 e−14	1.2664 e−13	6.1607 e−11
33	1.3277 e−13	2.6016 e−13	4.8189 e−13	3.9090 e−09
34	3.8754 e−15	3.7173 e−15	5.6945 e−15	2.5309 e−15
35	9.1937 e−15	5.3933 e−15	5.9242 e−15	3.8843 e−15
36	7.0017 e−15	1.1381 e−14	5.1544 e−15	7.0245 e−15
37	6.2601 e−14	7.5814 e−14	2.2697 e−14	3.0492 e−12
38	5.1983 e−14	2.5335 e−13	4.9573 e−14	2.8747 e+07
39	2.7223 e−15	1.1619 e−14	7.4048 e−15	2.8782 e−15
40	9.2429 e−15	1.0906 e−14	1.1375 e−14	1.1950 e−14
41	9.9618 e−15	5.3342 e−14	3.9347 e−14	1.1091 e−14
42	6.1524 e−14	5.2484 e−13	5.6221 e−13	6.0132 e−13
43	1.6310 e−13	2.0665 e−12	2.1802 e−12	6.0115 e−12
44	6.7513 e−15	4.6688 e−14	1.7129 e−14	9.3708 e−14
45	5.4463 e−15	3.8494 e−14	2.0670 e−14	1.1650 e−13
46	1.3952 e−14	4.2139 e−14	2.7587 e−14	1.2530 e−13
47	9.2145 e−14	2.4008 e−13	8.0347 e−13	1.2574 e−12
48	1.3591 e−13	2.2192 e−12	1.0772 e−12	5.2213 e−12

Table 8.14: Unbalanced double shift version: backward error measure (8.2).

No.	AMVW	DHSEQR	DGEEV	CGXZ
1	1.7383 e−15	1.2337 e−14	1.5451 e−15	2.4046 e−14
2	1.2141 e−13	8.7755 e−14	4.2634 e−15	2.8220 e−14
3	4.1017 e−12	9.4995 e−12	5.5798 e−15	6.9387 e−14
8	1.0908 e−15	3.3128 e−15	2.8280 e−15	1.8422 e−14
9	1.4707 e−11	1.8488 e−11	2.4582 e−15	4.2897 e−14
12	2.3391 e−15	7.7783 e−13	4.1584 e−16	1.0812 e−14
15	4.6325 e−11	2.2070 e−03	3.4985 e−10	4.1042 e−12
16	7.6627 e−06	4.0016 e−07	1.2261 e−09	2.4671 e−04
18	4.7103 e−16	1.3945 e−31	1.3945 e−31	7.0711 e−21
19	8.4853 e−16	2.8284 e−16	4.2426 e−16	8.4853 e−16
20	9.9516 e−17	0.0000 e+00	2.9855 e−16	0.0000 e+00
21	5.5585 e−15	9.8398 e−13	2.7586 e−17	2.7586 e−17
22	4.3034 e−15	4.3103 e−19	2.7586 e−17	3.1413 e−11
28	3.9028 e−15	1.7981 e−14	2.9271 e−15	1.1011 e−14

Table 8.15: Balanced double shift version: backward error measure (8.2).

$\|\,a\,\|_2$	AMVW	DHSEQR
1.0 e+00	7.3027 e−15	9.5340 e−15
1.0 e+01	5.9541 e−14	1.8201 e−14
1.0 e+02	1.6705 e−14	1.3158 e−14
1.0 e+03	9.8356 e−15	9.0239 e−15
1.0 e+04	7.1616 e−15	1.1320 e−14
1.0 e+05	5.9621 e−15	9.1007 e−15
1.0 e+06	6.3990 e−15	8.4219 e−15
1.0 e+07	9.9366 e−15	1.3407 e−14
1.0 e+08	6.0114 e−15	1.2528 e−14
1.0 e+09	9.0966 e−15	1.0999 e−14
1.0 e+10	4.8209 e−15	2.2653 e−14
1.0 e+11	1.0891 e−14	1.4562 e−14
1.0 e+12	6.7457 e−15	1.4330 e−14

Table 8.16: Backward stability (relative residual) for large values of $\|\,A\,\|_2$

For a second experiment we choose again random coefficients, but now only scale the a_0. The results in Table 8.17 show that making a_0 small causes no loss of backward stability. Of course, these simple examples do not prove that cases where large $\|\,A\,\|_2$ or small $|a_0|$ cause problems will never be found.

9. Conclusions. We have presented a fast and backward stable algorithm to compute the roots of a polynomial presented in monomial basis form. The algorithm is Francis's implicitly-shifted QR algorithm applied to a special representation of the companion matrix consisting of $3n-1$ rotators. Thus the memory requirement is $O(n)$. The flop count is $O(n)$ per iteration or $O(n^2)$ overall. Extensive tests indicate that the new algorithm is about as accurate as the (slow) Francis algorithm applied

$\lvert a_0 \rvert$	AMVW	DHSEQR
1.0 e−07	9.4161 e−15	1.0000 e−14
1.0 e−06	1.3281 e−14	1.3274 e−14
1.0 e−05	9.9456 e−15	7.6148 e−15
1.0 e−04	8.3509 e−15	1.9899 e−14
1.0 e−03	5.8908 e−15	1.8425 e−14
1.0 e−02	1.2840 e−14	1.0824 e−14
1.0 e−01	5.6900 e−15	1.2025 e−14
1.0 e+00	8.8024 e−15	1.8493 e−14
1.0 e+01	5.0423 e−15	2.9675 e−14
1.0 e+02	1.1126 e−14	9.6218 e−15

Table 8.17: Backward stability (relative residual) for small values of a_0

directly to the companion matrix. It is faster than other fast algorithms that have been devised for this problem, and its accuracy is comparable or better.

Acknowledgments. The authors thank Vanni Noferini for providing the polynomials 15 and 16, which proved to be quite challenging for some of the methods.

REFERENCES

[1] T. Aktosun, D. Gintides, and V. G. Papanicolaou, *The uniqueness in the inverse problem for transmission eigenvalues for the spherically symmetric variable-speed wave equation*, Inverse Problems, 27 (2011), p. 115004.

[2] J. Aurentz, R. Vandebril, and D. S. Watkins, *Fast computation of the zeros of a polynomial via factorization of the companion matrix*, SIAM Journal on Scientific Computing, 35 (2013), pp. A255–A269.

[3] ———, *Fast computation of eigenvalues of companion, comrade, and related matrices*, BIT, 54 (2014), pp. 7–30.

[4] R. Bevilacqua, G. M. Del Corso, and L. Gemignani, *A CMV–based eigensolver for companion matrices*, June 2014.

[5] D. A. Bini, P. Boito, Y. Eidelman, L. Gemignani, and I. Gohberg, *A fast implicit QR eigenvalue algorithm for companion matrices*, Linear Algebra and its Applications, 432 (2010), pp. 2006–2031.

[6] D. A. Bini, F. Daddi, and L. Gemignani, *On the shifted QR iteration applied to companion matrices*, Electronic Transactions on Numerical Analysis, 18 (2004), pp. 137–152.

[7] D. A. Bini, Y. Eidelman, L. Gemignani, and I. Gohberg, *Fast QR eigenvalue algorithms for Hessenberg matrices which are rank-one perturbations of unitary matrices*, SIAM Journal on Matrix Analysis and Applications, 29 (2007), pp. 566–585.

[8] D. A. Bini and G. Fiorentino, *Design, analysis, and implementation of a multiprecision polynomial rootfinder*, Numerical Algorithms, 23 (2000), pp. 127–173.

[9] D. A. Bini, G. Fiorentino, L. Gemignani, and B. Meini, *Effective fast algorithms for polynomial spectral factorization*, Numerical Algorithms, 34 (2003), pp. 217–227.

[10] P. Boito, Y. Eidelman, and L. Gemignani, *Implicit QR for rank-structured matrix pencils*, BIT, 54 (2013), pp. 85–111.

[11] P. Boito, Y. Eidelman, L. Gemignani, and I. Gohberg, *Implicit QR with compression*, Indagationes Mathematicae, 23 (2012), pp. 733–761.

[12] A. Böttcher and M. Halwass, *Wiener–Hopf and spectral factorization of real polynomials by Newton's method*, Linear Algebra and its Applications, 438 (2013), pp. 4760–4805.

[13] S. Chandrasekaran, M. Gu, J. Xia, and J. Zhu, *A fast QR algorithm for companion matrices*, Operator Theory: Advances and Applications, 179 (2007), pp. 111–143.

[14] F. De Terán and F. M. Dopico, *Low rank perturbation of regular matrix polynomials*, Linear Algebra and its Applications, 430 (2009), pp. 579–586.

[15] S. Delvaux, K. Frederix, and M. Van Barel, *An algorithm for computing the eigenvalues of block companion matrices*, Numerical Algorithms, 62 (2013).
[16] A. Edelman and H. Murakami, *Polynomial roots from companion matrix eigenvalues*, Mathematics of Computation, 64 (1995), pp. 763–776.
[17] Y. Eidelman, L. Gemignani, and I. C. Gohberg, *Efficient eigenvalue computation for quasiseparable Hermitian matrices under low rank perturbation*, Numerical Algorithms, 47 (2008), pp. 253–273.
[18] Y. Eidelman, I. Gohberg, and I. Haimovici, *Separable Type Representations of Matrices and Fast Algorithms – Volume 2: Eigenvalue Method*, no. 235 in Operator Theory: Advances and Applications, Springer Basel, 2013.
[19] J. G. F. Francis, *The QR Transformation a unitary analogue to the LR transformation–Part 1*, The Computer Journal, 4 (1961), pp. 265–271.
[20] ———, *The QR Transformation–Part 2*, The Computer Journal, 4 (1962), pp. 332–345.
[21] N. J. Higham, *Accuracy and Stability of Numerical Algorithms*, SIAM, 1996.
[22] M. A. Jenkins and J. F. Traub, *Principles for testing polynomial zerofinding programs*, ACM Transactions on Mathematical Software, 1 (1975), pp. 26–34.
[23] T. Mach and R. Vandebril, *On deflations in extended QR algorithms*, SIAM Journal on Matrix Analysis and Applications, 35 (2014), pp. 559–579.
[24] C. B. Moler, *Cleve's corner: Roots - of polynomials, that is*, The Mathworks Newsletter, 5 (1991), pp. 8–9.
[25] *MPFUN - multiprecision software*. http://www.netlib.org/mpfun/, 2005.
[26] K.-C. Toh and L. N. Trefethen, *Pseudozeros of polynomials and pseudospectra of companion matrices*, Numerische Mathematik, 68 (1994), pp. 403–425.
[27] M. Van Barel, R. Vandebril, P. Van Dooren, and K. Frederix, *Implicit double shift QR-algorithm for companion matrices*, Numerische Mathematik, 116 (2010), pp. 177–212.
[28] P. Van Dooren and P. Dewilde, *The eigenstructure of an arbitrary polynomial matrix: Computational aspects*, Linear Algebra and its Applications, 50 (1983), pp. 545–579.
[29] R. Vandebril and G. M. Del Corso, *An implicit multishift QR-algorithm for Hermitian plus low rank matrices*, SIAM Journal on Scientific Computing, 32 (2010), pp. 2190–2212.
[30] D. S. Watkins, *The Matrix Eigenvalue Problem: GR and Krylov Subspace Methods*, SIAM, Philadelphia, USA, 2007.
[31] ———, *Fundamentals of Matrix Computations*, Pure and Applied Mathematics, John Wiley & Sons, Inc., New York, third ed., 2010.
[32] ———, *Francis's algorithm*, American Mathematical Monthly, 118 (2011), pp. 387–403.
[33] J. H. Wilkinson, *The Algebraic Eigenvalue Problem*, Numerical Mathematics and Scientific Computation, Oxford University Press, New York, USA, 1988.
[34] P. Zhlobich, *Differential qd algorithm with shifts for rank-structured matrices*, SIAM Journal on Matrix Analysis and Applications, 33 (2012).